# NJC

Accepted Manuscript

This is an *Accepted Manuscript*, which has been through the RSC Publishing peer review process and has been accepted for publication.

Accepted Manuscripts are published online shortly after acceptance, which is prior to technical editing, formatting and proof reading. This free service from RSC Publishing allows authors to make their results available to the community, in citable form, before publication of the edited article. This *Accepted Manuscript* will be replaced by the edited and formatted *Advance Article* as soon as this is available.

To cite this manuscript please use its permanent Digital Object Identifier (DOI®), which is identical for all formats of publication.

More information about *Accepted Manuscripts* can be found in the **Information for Authors**.

Please note that technical editing may introduce minor changes to the text and/or graphics contained in the manuscript submitted by the author(s) which may alter content, and that the standard **Terms & Conditions** and the **ethical guidelines** that apply to the journal are still applicable. In no event shall the RSC be held responsible for any errors or omissions in these *Accepted Manuscript* manuscripts or any consequences arising from the use of any information contained in them.

RSC Publishing

www.rsc.org/njc
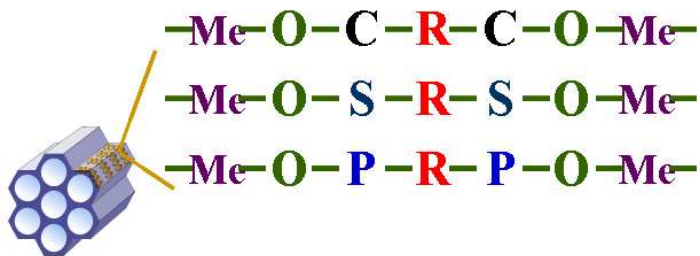
An overview of the recent progress in the designed synthesis, modification and multifunctional applications of mesoporous non-siliceous inorganic-organic hybrid materials including metal phosphonates, carboxylates and sulfonates is presented in this Perspective article.

PERSPECTIVE

Mesoporous Non-Siliceous Inorganic-Organic Hybrids: A Promising Platform for Designing Multifunctional Materials

**Yun-Pei Zhu,[a] Tie-Zhen Ren[b] and Zhong-Yong Yuan*[a]**

Recent progress in mesoporous materials has been extended to chemically designed non-siliceous inorganic-organic hybrid materials including metal phosphonates, carboxylates and sulfonates. Well-defined mesoporosity, mesophase and micro-/macroscopic morphology can be successfully obtained and effectively adjusted by the judicious control of the synthesis systems. A considerable amount of organic

10 functional groups can be homogeneously integrated in the hybrid framework through facilely employing various organic coupling molecules, exhibiting the pristine functionalities and the potentials of being further modified. This has resulted in multifunctional porous materials with particular and novel properties and broadened their application region beyond the traditional use as catalysts and adsorbents, even can be set to contribute to the developments in the fields ranging from energy storage and

15 conversion to medical diagnosis and therapy.

1 Introduction

With the rapid development of human civilization, energy, environmental and health issues have received increasing attention. Coal, petrol and natural gas as traditional fossil fuels

20 are exceedingly depleted, accompanied with emission of harmful chemicals to the atmosphere. In response to the energy crisis and environmental contaminations, clean energy and sustainable development are the basic principles. Where the core ideology lies is the invention and development of advanced multifunctional

25 materials, which is essential for alternative and renewable sources, and the abatement of harmful substances. Thus, porous materials with the superiority of diverse compositions and large surface areas have gained popularity, and they have exhibited broad applications for catalysis, adsorption, separation, energy storage,

30 and sensing to biotechnology.[1-4]

Nanoporous materials as a subset of nanostructured materials possess the ability to interact with atoms, ions, molecules, and even larger guest molecules not only at the surface but also throughout the bulk of the materials.[5,6] Relative to microporous

35 and macroporous materials, mesoporous materials have attracted more and more research interest and shown great potentials in many fields due to their outstanding properties such as approximate pore diameters, high surface areas, tunable porosity,

50 alternative pore shape, abundant compositions.[7-14] The most classical and famous mesoporous materials are silica-based materials, such as M41S family,[15] SBA series,[16] and their related mesostrucures[17,18]. However, it is frustrated that the use of pure inorganic silica-based materials is limited to physical properties

55 concerned with catalytic supports and adsorbents, showing insufficiency with respect to the low mechanical strength and the difficulties in post-modification or functionalization. The introduction of organic moieties into the framework of silica-based materials is an alternative way in nanomaterial

60 investigation. Periodic mesoporous organosilicas (PMOs), which contain organic groups such as siloxane bridges in the silica network, have been the most widely investigated hybrids.[19,20] The predominant process in the formation of siliceous hybrid mesoporous materials during the sol-gel procedure is the

65 incorporation of organic groups via hydrolysis and polymerization by using organically modified silanes. The homogeneous distribution of organic bridges both in the wall and
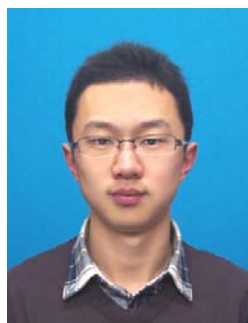
Yun-Pei Zhu received his BSc degree in 2011 at Henan Polytechnic University. He is currently a graduate student under the

40 *supervision of Prof. Zhong-Yong Yuan at Nankai University. His current research relates to the rational design of porous inorganic-organic hybrid materials for*

45 *applications in catalysis, adsorption, separation and biosensing.*

Tie-Zhen Ren obtained her PhD degree from the University of Namur,

70 *Belgium in 2005. After two-year postdoctoral research at Stockholm University, Sweden, she joined the faculty of the Hebei University of Technology in 2007, where she is*

75 *currently Professor in Chemical Technology. Her group's research areas include nanoporous photoelectrochemical materials and metal-organic frameworks.*

on the surface is fascinating and valuable from the viewpoint of materials and chemistry.[21] However, besides the limited choice and high cost of the precursors of organosilicane, functionalization of organosilicas is confined to the physical properties concerned with adsorption, ion-exchange and catalysis. The exploitation of hybrid materials has thus been extended to non-silica-based inorganic-organic hybrid materials.

Chemically designed non-siliceous inorganic-organic mesoporous hybrids, in which metal sulfonates, carboxylates and phosphonates represent the three members of the family, are considered to be promising candidates for environmentally friendly and multifunctional materials.[22,23] Differing from traditional inorganic porous materials, chemically designed organic-inorganic hybrids are not simple physical mixtures of inorganics and organics, but are nanocomposites composed of alternative organic-inorganic hybrid frameworks at the molecular scale, presenting a combination of properties from the alternative inorganic units and organic moieties in the framework.[24] Different dimensions and reactivities of the bridging molecules lead to distinct structures and stabilities of the resultant hybrids. Because of a variety of the available organic acid linkages and their derivatives (*i.e.*, salts or esters), and various metallic precursors, the physicochemical properties of hybrid frameworks can be designed and further modified adequately through using different metal ions and organic bridging molecules.[25] Not only the hydrophobic/hydrophilic and acid/alkaline natures of the pore surface could be adjusted, but also the homogeneous introduction of functional binding sites into the framework could be realized.[26] The post-modification of these hybrids was improved, due to the easy condensation reaction between the grafting molecules and the organic moieties in the hybrid network. It is well-known that the distribution of pore sizes, shapes and dimensions in mesoporous materials directly are related to their capabilities to perform the desired functions in a particular application. By ingenious selection of synthesis systems and technology, the pore width, mesophase, crystallization of the pore walls and morphology of the mesoporous non-siliceous hybrids can be effectively controlled. And thus mesoporous metal-organic hybrids have been widely utilized in adsorption, separation, catalysis, photochemistry, and biochemistry owing to their high surface area, large pore volume, adjustable porosity, easy handling, low-cost of manufacture, and intriguing surface properties.[25]

Recently, Xuan *et al.*,[27] Fang *et al.*,[28] and Song *et al.*[29] have presented their reviews of mesoporous carboxylate-based metal-organic framework (MOFs). Kimura reviewed the surfactant-assisted synthetic processes of mesoporous organophosphonate hybrids from bisphosphonates and briefly introduced the potential applications.[30] The present perspective summarizes and highlights recent progress of mesoporous non-silica-based hybrid materials with controllable composition and structural properties, including metal sulfonates, carboxylates, phosphonates and some current research hot topic MOFs. The pivotal factors in rational synthesis and design of mesoporous non-siliceous hybrids were discussed in detail. The modification and the representative applications of these innovative materials were also clarified, which aims at attracting more research interests to make the mesoporous non-siliceous hybrids fit the qualification in practical applications in near future.

2 Synthesis

2.1 Template-free self-assembly synthesis strategy

In recent years, researchers have paid much attention on the synthesis of porous nanostructured hybrid materials through template-free self-assembly strategy, which do not need the use of the pre-formed templates or structure-directing agents. These routes usually initiate the assembly from the interactions between the precursor molecules, and the ordered attachment allows the formation of porous morphologies.

Microporous inorganic-organic hybrid materials are often known as crystalline MOFs, which involve the strong and regular coordination of metal ions and organic linkage moieties, thus yielding porous framework structures. Compared with typical microporous metal carboxylates, metal phosphonates have exhibited higher chemical and thermal stability due to the strong affinity and chelation of organophosphonic linkers to metal ions. Phosphonate hybrids often come up in the form of dense layered motifs, which evolved into the field of inorganic-organic hybrids by appending the organic pillars off the rigid inorganic layers.[31] It should be recognized that the pillars are too crowded and insufficient free space remains in the interlayer region, and no or poor porosity is expected to be present.[32] Several tactics have been adopted to create porosity in the metal phosphonate frameworks. The first route is substitution of aryl biphosphonic acid by some non-pillaring groups, such as phosphoric, phosphors, and methylphosphonic acids, leading to the presence of interlayer pores and the increase of surface area.[33] Although a porous phosphonate can be obtained, the problem of this approach is that replacement is random and uncontrollable, and the structural characterization and a narrow pore size distribution are still challenges. Secondly, the geometry of a large and multidimensional polyphosphonic bridging molecule would disfavour the formation of the layered motif and thereby necessitate an open framework. A third approach would be to attach a second functional group to the phosphonate ligand to coordinate with metal centers and disrupt the structure away from layers.[34]

Zhong-Yong Yuan received his BSc degree from Zhejiang Normal University in 1990, and obtained his MSc and PhD degrees from Nankai University in 1996 and 1999, respectively. After his postdoctoral research at the Institute of Physics, Chinese Academy of Sciences, he joined the Laboratory of Inorganic Materials Chemistry at the University of Namur, Belgium in 2001. In 2005, he was engaged as a Professor in Nankai University. His research interests are mainly focused on the self-assembly of hierarchically nanoporous and nanostructured materials for energy and environmental applications. He is coauthor of 180 ISI publications, 3 book chapters and 10 patents.

Metal sulfonate networks have been studied considerably less than other kinds of hybrid materials because of the relatively weak coordination interactions between sulfonate anions and metal cations, which make the frameworks not sufficiently robust to sustain permanent porosity.[35] The chelation capacity of organic linkages to metal ions usually follows the sequence of phosphonates > carboxylates > sulfonates. Metal sulfonates have been considered as potential analogues of layered metal phosphonates.[36] The rigid inorganic layers provide scaffolds of regular anchor points for pendant organic groups. In keeping with the theme of using larger cores with regard to the porous phosphonates to disperse the crossing sulfonate groups, the pillaring group, 1,3,5-tris(sulfomethyl)benzene, could be envisioned to open channels between the layers of a metal sulfonate.[37]

2.1.1 Ligand extension

Crystalline hybrids are constructed from the regular linkages of metal centers and organic groups, which can achieve well-defined pores, high porosity and surface area. Nevertheless, their pore sizes are typically restricted to the microporous regime. Thus, the synthesis of mesoporous hybrids is envisioned to improve the transmission capability of the pores while facilitating practical applications that require bulky molecules diffusion.[38] Using extended ligands or bulky secondary building blocks is an apparent strategy. Disappointedly, linker expansion tends to lead to reduced surface areas and pore sizes due to the consequent interpenetrated structures, and dramatically reduce the stability of the framework upon solvent removal from the porous hosts.[39] An elaborately designed ligand with hierarchical functional groups, 4,4',4''-s-triazine-1,3,5-triyltri-p-aminobenzoate, could be devised to extend the linkers while inhibiting interpenetration and reinforcing the framework against disintergration upon guest removal.[40] The mesoporous MOF was prepared through a one-pot solvothermal method, followed by stabilization of at pH values around. The amino groups in the ligand were prearranged so that they would not participate in the framework formation but could accept protons after the network was generated, giving rise to a stable mesoporous MOF up to 300 ºC. N_2 sorption isotherm exhibited a typical type IV behavior, and the XRD confirmed the open channels were identical in size and as large as 22.5 × 26.1 Å. Similarly, Schröder *et al.* reported the synthesis of (3,24)-connected mesoporous framework NOTT-119 by adopting a nanosized C_3-symmetric hexacarboxylate linker, presenting a high surface area of 4118 m^2 g^{-1} and pore sizes in the range of 2.4 – 4.5 nm.[41] The hybrid framework is stable up to 315 ºC. When the dimension of the linker was enlarged beyond the point, the network could no longer hold stability to thermal treatment and suffer disruption of the structure owing to surface tension effects. A homologous series of palindromic oligophenylene derivatives terminated with α-hydroxy-carboxylic acid functions were targeted to afford linear and robust building blocks for expanding the pore size to up to 9.8 nm,[42] which is the largest channel via ligand-expanding method to date. All members had non-interpenetrating structures and exhibited robust architectures, as evidenced by their permanent porosity and high thermal stability.

Recently, a multidimensional ligand, tetrakis-1,3,5,7-(4-phosphonatophenyl)adamantine, which could impede the formation of a close-packed arrangement of organic molecules in an inorganic-organic hybrid framework, was used to fabricate mesoporous metal phosphonate materials.[43] The preparation was accomplished through a non-hydrolytic condensation process between the tetraphosphonic acid and titanium (IV) isopropoxide in DMSO, permitting the generation of mesopores. N_2 sorption experiments revealed the presence of mesopores of about 3.8 nm accompanied with a surface area of approximately 550 m^2 g^{-1}. Mesoporous vanadium phosphonates could also be obtained by using the same method, exhibiting a BET surface area of 118 m^2 g^{-1} and a Barrett-Joyner-Halenda (BJH) pore diameter of 3.8-3.9 nm.[44] FT-IR and XPS as well as elemental analysis suggested that the phosphonate claw molecules were most likely connected in the form of $ArP(O)O_2V_2O_2(O)PAr$.

2.1.2 Microemulsion method

Although ligand extension is an effective way to expand micropores to mesoporous regime in the hybrid materials, most complicated organic linkers are not commercially available and in order to gain them, complicated fabrication progresses are generally required. More recently, a new method to prepare mesorporous hybrid metal phosphonates by employing microemulsions was reported by Yuan and co-workers.[45] Mesostructured pores of several nanometers in size existed in the vicinity of the surface in a wormhole-like assembly (2.5-5.8 nm), whereas in the core, close to the wormhole-like mesoporous surface layers of the particle, a new mesocellular foam structure (8-10 nm) similar to the previously reported mesostructured cellular foam (MCF) silica materials[46] was observed (Fig. 1). During the period of synthesis, hydrolysis of titanium tetrabutoxide in ethylenediamine-tetra(methylene phosphonic acid) aqueous solution resulted in the rapid formation of nanometer-sized titanium phosphonate and butanol molecules at the same time. Thereafter, microemulsion drops formed in the multi-component system of alkoxide/organophosphonate-alcohol-water while stirring. The phosphonate sols aggregated along with the microemulsions, evolving to mesocellular foam structure. The interactions between the sols caused the formation of mesostructured nanoclusters of several nanometers in size. At this stage, due to the presence of large amount of butanol byproducts, the reaction mixture transferred to phosphonate-based mesophases and water/alcohol domains by microphase separation, induced by aging, leading to discrimination of them and even some macrovoids. If 1-hydroxy-ethylidene-1,1-diphosphonate was chosen as organic precursors, according to microemulsion methodology, the interfacial polymerization of titanium phosphonate sols and titanium-oxo clusters resulted in the formation of mesostructured hybrid nanorods with a length of 80-150 nm and a thickness of 18-38 nm.[47] The multipoint BET surface area was 257 m^2 g^{-1}, accompanied with a BJH pore size of 2.0 nm and a total pore volume of 0.263 cm^3 g^{-1}.

2.1.3 Nanocrystal self-assembly

The preparation of single-sized porous hybrid materials from angstroms to micrometers has been an interesting research area in the past several decades.[48] However, materials presenting multiscale or multimodal porosity show even a higher interest due to the enhanced mass transport through the larger pores and maintenance of a specific surface area on the level of fine pore systems, which is a central point of many processes concerning accessibility, especially catalysis, adsorption, optics and sensing.[49,50] Expanding the pore width of the crystalline inorganic-organic hybrid via a ligand extension method has been
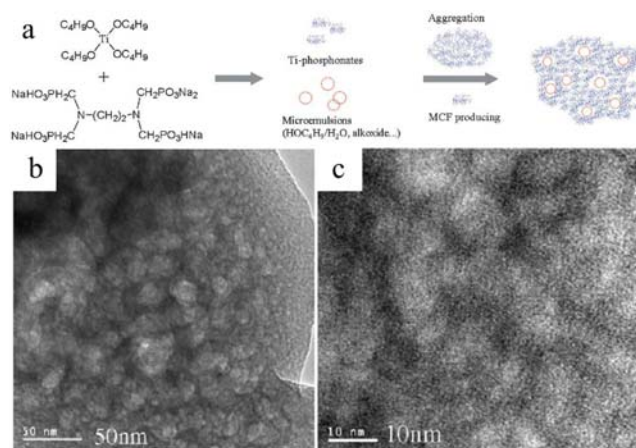
Fig. 1 Proposed formation mechanism of titanium phosphonates with both wormhole-like mesopores and MCF structures (a), and the corresponding TEM images (b, c). Reprinted with permission from ref. 45.

demonstrated.[51] But the creation of larger pores through ligand-extension usually involves the expense of the loss of micropores. Moreover, the ordered nanostructures or pores could only be retained for small mesopore sizes or constricted cages.[52] Yue *et al.* reported a surfactant-free methodology for the synthesis of Zn-MOF-74 with hierarchical micro-/mesoporosity using 2,5-dihydroxy-1,4-benzenedicarboxylate.[53] The synthesis was proceeded at room temperature to restrict the crystallization, and finally nanosized MOF-74 crystals were formed. The acetate from inorganic precursors could accelerate the crystal generation through ligand-exchange process[54] that would not be expected to happen with the conjugate bases of strong acids (*e.g.*, Cl^-, SO_4^{2-}, and NO_3^-). The precipitate materials were composed of discrete MOF nanoparticles embedded in amorphous matrix, which exhibited large interpartical mesopores in the 2-20 nm range and intrapartical micropores with a maximum at ~ 1.1 nm confirmed by N_2 sorption and TEM observation.
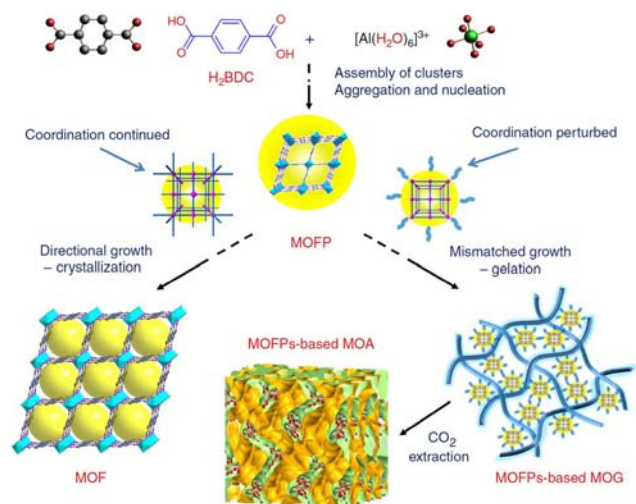
Fig. 2 Schematic representation of the formation of highly crystalline MOF *versus* MOA. Reprinted with permission from ref. 58.

Aerogels are well-known because of versatile porosity, low density, and high internal surface area, but the design of aerogels is still rudimentary due to a large disorder in the structure and the insufficient prediction of gelation behavior.[55] Noticeably, metal-ligand coordination and other supramolecular forces (*e.g.*, H-bonding, π-π stacking, and van der Waals interactions) are emerging as effective driving forces to gelation, offering metal-organic gels (MOGs) as a novel class of functional soft materials.[56,57] On the basis of the inherent correlations between MOFs and MOGs, Li *et al.* reported a general synthetic route for the fabrication of hierarchically porous metal-organic aerogels (MOAs) via MOG formation from the self-assembly of precursor (Fig. 2).[58] Typically, the strong metal-ligand coordination interactions impel the metal ions and organic linkages to assemble into MOF clusters, which then polymerize to MOF nanoparticles with well-defined microporosity. Under the reaction conditions that favored the consistent epitaxial growth or oriented attachment,[59,60] the further crystallization of MOF subunits could lead to bulky MOFs. Moderate heating represented a key factor in mismatched growth or cross-linking of preformed MOF particles and then triggering the gelation of proper solvents (mainly ethanol). The careful removal of the solvents by sub/supercritical CO_2 extraction left hierarchically porous MOAs based on MOGs. The N_2 sorption isotherms are between type I, characteristic of microporous materials, and type IV, indicative of mesoporous materials. The texture and porosity could be easily adjusted by changing precursor concentrations.

Zhao and co-workers reported the synthesis of stable bicontinuous hierarchically porous MOFs (ZIF-8 and HKUST-1) with the assistance of a coordination regulating agent.[61] The resulting materials resembled the microstructures of bicontinuous silica aerogels, composed of branched fibrous network of interconnected ~40 nm sized microporous nanocrystallites. Besides the intrinsic micropores, the prepared ZIF and HKUST-1 exhibited aerogel-like textural interparticular voids from 2 to 100 nm, encompassing the meso- and macro-porous regions that were absent in the single crystal forms.

Mesoporous even macroporous non-siliceous hybrids could be obtained through self-assembly approach in the absence of any templates or surfactants. No matter using linkage extension, microemulsion or nanocrystal self-assembly methodologies, they usually involve weak interactions among the hybrid nano-building blocks. Other interactions such as hydrogen bond, hydrophobicity-hydrophobicity interaction and π-π stacking can also direct the spontaneous formation of mesoporous non-siliceous materials with fascinating porosity, structures and stability, which are mainly dependent on the synthesis conditions.

2.2 Surfactant-mediated synthesis strategy

Surfactant- or template-free approach has been proven to be a valuable way to obtain hybrid inorganic-organic materials presenting porosity from micropores to macropores. Nonetheless, this method cannot afford the valid capability to adjust the porosity, texture, and even morphologies on demand. As to some kinds of potential applications, such as separation and recognition of large molecules, catalyst supports, and dye adsorption, the existence of mesopores is much more preferable than micropores and macropores to some certain extent. Using supramolecular templates to synthesize ordered mesoporous materials have received increasing attention in the last decades, due to the periodically aligned pore systems, uniform pore size in the mesoscale region, high surface area, controllable mesophase, and abundant framework compositions, and found diverse

applications in the fields of adsorption, separation, catalysis, biosensing, and energy storage and conversion.[62] Surfactant-induced route for the formation of mesopores can be classified into two types.[63] The first ones are termed as hard-templates or nanocasting, which are the prepared mesoporous materials with solid frameworks, including carbons, polymer beads, and silicas. However, the prepared materials often have a wider pore size distribution than that of the pristine replicas; and multiple preparation procedure at the sacrifice of the costly hard templates makes it expensive, complicated, and consequently unsuitable for large-scale production and industrial applications. Meanwhile, the template removal always involve the strong acids, bases, and high-temperature calcination, which cause it favorable for the synthesis of special mesoporous materials, for instance, metal sulfides and oxides,[64,65] carbons,[66-67] and silicon carbides,[68] while not suitable for the cases of hybrid materials. Soft-templating methodology, which is usually referred to "soft" molecules including ionic surfactants (*e.g.*, CTAB) and nonionic block copolymers (*e.g.*, F127), has received much attention. In comparison with the nanocasting method, the entire procedure of soft-template is low-cost, facile, convenient, effective, and promising for large-scale production. More importantly, the mesophase formation depends on the temperature, type of solvent, ionic strength and pH, and the nature of the template molecules (hydrophobic/hydrophilic volume ratio, hydrophobic length, *etc*.), which make the pore structure and surface properties easy to be tuned. Thus, the preparation of mesoporous hybrid materials through soft-template strategy will be discussed detailedly in the following parts.

2.2.1 Synthesis mechanism

Since the liquid-crystal templating theory was proposed, unprecedented amounts of studies concentrated on the synthesis, modifications and applications of mesoporous materials have been sprung up. Mesoporous inorganic-organic hybrids are of no exception. Proverbially, surfactants consisting of hydrophilic heads and hydrophobic tails can assemble into micelles at a concentration higher than the critical micelle concentration under the driving force of hydrophobic interactions. And lyotropic liquid can provide an organized scaffold. The formed oligomers from the condensation and polymerization of inorganic/organic precursors grow around the arranged surfactant micelles driven by the interactions (*e.g.*, electrostatic forces and hydrogen) between the surfactant molecules and the oligomers. After a further condensation and polymerization, the surfactants can be removed with leaving a mesoporous structure. According to the synthetic conditions, chemical diversity of composite mesoporous materials has been expanding during the last decades, with many synthesis pathways being demonstrated during the nucleation of the composite phase, such as direct surfactant-inorganic interaction (S^+I^-, S^-I^+, S^0I^0) and mediated interaction ($S^+X^-I^+$, $S^-X^+I^-$, $(S^0H^+)X^-I^+$).[69] The mesophase behaviors and pore width are dominated by the liquid-crystal scaffolds.

2.2.2 How to obtain periodic mesoporosity effectively?

Hybrid oligomers can be either generated during the reaction process or preformed before assembling with the surfactant micelles. The key factors for the assemblies to periodic mesophase include the control on the aggregation of precursors, the sufficient interactions between oligomers/precursors and surfactants, and in turn, proper size and charge of suitable building blocks.[70] For the synthesis of ordered mesoporous siliceous materials, it is relatively easy to gain chargeable hydrated silicate oligomers due to the undertaken hydrolysis of the inorganic precursors at a certain pH environment. In contrast, the uncontrollable hydrolysis and condensation for most non-siliceous inorganic precursors and the tendency to form crystalline products find it difficult in fitting the liquid-crystal template mechanism to produce stable and accessible long-range periodic mesostructures. The synthesis system is rather complicated, for instance, multi-inorganic precursors, solvents, acid or base to preserve the pH steady, and retainable chemical integrity and pre-formed mesostructures during the process of surfactant removal. In order to obtain ordered mesoporous hybrid materials, an appropriate system is necessary to prohibit or reduce the hydrolysis of inorganic sources and the coordination rates of metal ions and organic groups, and to enhance the interactions between surfactant scaffolds and charged oligomers.

Roy *et al.* prepared a family of alkyl pyrazinium surfactants that could tether to the Prussian blue (PB) precursors, enabling the isolation of a kinetically controlled mesostructrue.[71] The further reactions with $Na_3[Fe(CN)_5NH_3] \cdot 3H_2O$ gave an amphiphilic intermediates that templated the formation of mesostructured PB analogues. But the chemical binds between surfactant ionic heads and PB-type inorganic skeleton made it difficult to remove the surfactants. Direct cooperative self-assembly of metal ions, cationic surfactants and ligands with weak coordination acting sites to induce surfactants to overcome the lattice stability was accomplished by Li *et al.*,[72] resulting in mesostructured MOFs with amorphous wall. Also, the surfactant molecules could not be removed from the final MOF products.

Highly acid reaction system has been proven an efficient way to lower the hydrolysis of metal sources owing to the formation of large amounts of positively charged hybrid oligomers instantly. Kimura prepared highly ordered mesoporous aluminum organophosphonates by using alkyltrimethylammonium surfactants.[73,74] In the ethanol-water system, ordered hexagonal mesostructures could be gained through the reaction of aluminum chloride and alkylene diphosphonic acids under highly acidic conditions. However, the XRD patterns of the mesoporous materials showed a low ordering of the mesostructures. Elemental analysis indicated the presence of Cl^- anions in the frameworks. This revealed that the mesostructured materials were conducted through the $S^+X^-I^+$ or $(S^0H^+)X^-I^+$ pathway, demonstrating the impureness of the hybrid framework. The surfactant molecules accommodated in the mesopores could not be extracted by conventional acid treatment due to the less condensed and easily hydrolyzed networks, and thus calcination at 400 ºC was carried out. Oligomeric surfactants or triblock copolymers could also be used for the preparation of mesoporous aluminum phosphonates.[75]

Addition of organic solvents or organic chelates is another alternative approach to inhibit the hydrolysis. Haskouri *et al.* synthesized pure periodic mesoporous aluminum phosphonates and diphosphonates from aluminum "atrane" complexes, methylphosphonic, and ethylenediphosphonic acids through a S^+I^- surfactant-assisted cooperative mechanism by means of a one-pot preparative procedure.[76,77] A soft chemical extraction procedure enabled the opening of the pore system of the parent

mesostructured materials by exchanging the surfactant without the collapse of the mesostructure. The BET surface area of the mesoporous hybrid could reach up to 793 cm^2 g^{-1} accompanied with a narrow pore width distribution around 2.7 nm. This procedure was on the basis of the use of cetyltrimethylammonium bromide (CTAB) as a structure-directing agent and 2,2',2''-nitrilotriethanol as the complexing polyalcohol, which had proven its capability in controlling the rates of hydrolytic reactions of aluminum species in water-phosphoric acid media and the subsequent process of self-assembly in the presence of surfactant aggregates.[78]

Yuan's group reported the successful preparation of periodic mesoporous titanium phosphonate (PMTP-1) with bridged-organic linkers inside the framework via an autoclaving process followed by an evaporation-induced self-assembly (EISA) strategy.[79] To slow down the hydrolysis of titanium tetrachloride, the metallic precursors was dissolved in the ethanol previously to form TiOCH$_2$CH$_3$ complexes.[80,81] A cryosel bath was used to create a low-temperature condition as well to reduce the condensation speeds of the reactants. This could avert the generation of large titania or titanium phosphonate aggregations during the reaction process. It was found that highly ordered mesostructures were obtained when the pH value was sustained at a moderately acid according to the (S^{0}H$^+$)X$^-$I$^+$ mechanism, probably due to that newly formed gel was partially damaged in the strong acid system and that alkaline conditions led to a fast hydrolysis rate. The surface area, pore size, and pore volume were 1066 m^2 g^{-1}, 2.8 nm, and 0.83 cm^3 g^{-1}, respectively. This mechanism could be extensively applied to the formation of a series of periodic mesoporous metal phosphate and phosphonate materials with different structural phases in the presence of nonionic surfactants in acidic media.[82,83]

In recent years, ionic liquids (ILs), considered as tuneable and environmental friendly solvents, have attracted a lot of interest in the synthesis of novel materials. Zhang *et al.* synthesized well-ordered mesoporous MOF nanospheres constructed by a microporous framework in a system of ILs/surfactant combined with superficial CO$_2$.[84] The IL and surfactant were chosen as 1,1,3,3-tetramethylguanidinium acetate (TMGA) and *N*-ethyl perfluorooctylsulfonamide (EtFOSA), respectively. It has been shown that TMGA/EtFOSA/CO$_2$ microemulsions could be formed.[85] The surfactant molecules self-assembled into cylindrical micelles with the fluorocarbon chain directed towards the inside of the micelles, and CO$_2$ existed as a core of the micelles. Thereafter, the Zn(II) ions and 1,4-benzenedicarboxylic acid linked facilely around the formed micelles. And so, the mesoporosity was generated from the templating effect of surfactants, and microporosity was related to the intracrystalline cavities. The calculated sizes of mesopores and micropores were 3.6 and 0.7 nm, respectively, as well as a total surface area of 756 m^2 g^{-1}. The corresponding crystal structure could not be identified mainly owing to the small size of the nanoparticles.

An abundant variety of strategies have been taken out to effectively synthesize mesoporous non-siliceous hybrids. To efficiently mediate the coordination and condensation of organic linkers and inorganic species while increasing the interactions between surfactant scaffolds and the formed oligomers is the key factor. The removal of surfactant molecules to leave mesovoids in

the framework was preferred to use moderate measures including extraction by organic polar solvents and ion exchange, which could efficaciously prohibit the collapse of the mesoporous network.
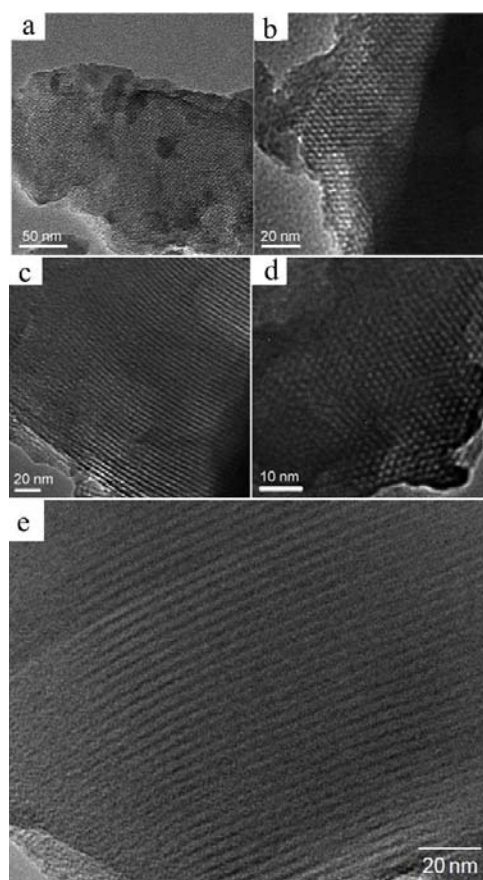
Fig. 3 TEM images of cubic (a, b), hexagonal (c, d) and lamellar (e) mesostructured phosphonates. Reproduced with permission from ref. 91 and 92.

2.2.3 The adjustment of mesostructures

The adjustment of mesostructures is still challenging in preparing periodic mesoporous hybrid materials, while it is a key step in regulating their physicochemical properties. A lot of factors could cause the phase transformation of the mesopores including the interactions between the organic and inorganic species,[86] the reaction temperature and time,[87] the addition of some inorganic additives,[88] the nature of surfactant that could be clarified using the molecular surfactant packing parameter,[89] the molar ratios of the surfactant and inorganic precursor[90], and so forth. Herein the molar ratios of the reactants were found to be critical to determine the final mesostructures of the hybrid materials, and different mesophases could be obtained by adjusting the amount of added reagents and surfactant. A synthesis condition map of periodic mesoporous titanium phosphonates with various phases has been explored.[91] The molar ratios of Ti/P should be fixed as 3:4 and 1:4 for hexagonal and cubic mesostructures under the experimental conditions, respectively, while mixed phases with poor pore periodicity also existed at these two Ti/P ratios (Fig. 3). It was easy to understand that the Ti/P ratio in hexagonal mesophases because one Ti atom was coordinated with four P atoms, whereas one P was coordinated with three Ti atoms and

also connected to one C atom. The P species was superfluous in cubic mesophases probably due to the existence of some P atoms with low-coordination state. By varying the molar ratios of CTAB/Ti, a general range for the synthesis of different
5 mesophases was confirmed, namely, in the region of $0.1<CTAB/Ti<0.4$ (Ti/P=3:4) for a hexagonal phase, at $0.4<CTAB/Ti<1.9$ (Ti/P=3:4, 1:4) for a mixed phase with poor pore regularity, and within the range of $1.9<CTAB/Ti<2.3$ (Ti/P=1:4) for a cubic phase, which was coincided with the
10 previously reported molecular surfactant packing parameter theory that the hexagonal phase is formed at a low surfactant/inorganic species ratio and the cubic phase formed at a high ratio.[89] Lamellar mesostructured aluminum organophosphonate (Fig. 3e) with unique inorganic-organic
15 hybrid network could be synthesized from the reactions of aluminum triisopropoxide with methylene disphosphonic acid with the assistance of alkyltrimethylammonium when the corresponding atomic ratios decreased to Al/P/CTAB = 1:4:2.[92] The organic diphosphonic bridges were embedded in the
20 integrated hybrid sheets with surfactant micelles inserted between the sheets. The removal of the surfactant would lead to the irreversible collapse of lamellar phase, which signified that it had limited values from the practical applications point of view.

For mesoporous siliceous materials, the curvature of
25 mesostructures increases from lamellar via hexagonal to cubic phases, and the control of mesostructure is commonly dependent on the hydrophilicity/hydrophobicity ratio and the molecular weight of the surfactants.[93,94] The ease in tuning the surfactant composition via living polymerization paves the way to adjusting
30 the mesophase. Initially, it is considered that lower hydrophilicity/hydrophobicity ratios lead to the formation of mesophases with small curvatures (*e.g.*, lamellar), and high ratios are favorable for the generation of the ones with large curvatures (*e.g.*, hexagonal and cubic).[95] For example, the utilization of
35 $EO_{80}PO_{30}EO_{80}$ with high EO:PO ration led to the preferential formation of cubic $Ia\bar{3}d$ phases and cage-type ones with $Fm\bar{3}m$ and $Pm\bar{3}m$ structures.[96,97] In the cases of non-silica-based hybrid materials, the hexagonal mesophases are usually preferred in spite of the molecule structures and compositions. This may be
40 due to the fact that the hybrid network condensed incompletely, and the arrangement of surfactant scaffolds containing inorganic species attached at the hydrophilic portions can make a difference from those of silica-based mesostructures.[98] Furthermore, the complex coordination chemistry between metal ions and organic
45 bridges and the weak interactions among the organic components may devote to forming relatively stable hexagonal phases.

2.2.4 The control over the pore sizes
Pore size control of mesoporous materials is a vital issue as it is directly bound up with the applications. The pore sizes are mainly
50 relied on the hydrophobic volumes of the template molecules. With this in mind, the intentional selection of surfactants with various lengths of hydrophobic chains can make the pore size control come true. Using soft templates with low molecular weight such as CTAB and oligomeric surfactants (*e.g.*, $C_{16}EO_{10}$
55 and $C_{16}EO_{20}$), the pore diameters usually distributed in the range of 2-4 nm.[73-75,79,82,83] The pore width could be largely expanded to 6.0-10 nm if triblock copolymers ($EO_{80}PO_{30}EO_{80}$, $EO_{106}PO_{70}EO_{106}$, and $EO_{20}PO_{70}EO_{20}$) were employed.[75,99,100]

Colloidal templating of polystyrene-*block*-poly(oxyethylene)

60 (PS-*b*-PEO) was newly developed for the fabrication of porous aluminum phosphonates with large spherical pores.[101] PS-*b*-PEO was dissolved in a mixed of THF and ethanol by the presence of water to form spherical aggregates and then mixed with precursor solutions before preparation. Then the mixed solutions were
65 spray-dried at different temperatures from 110 to 230 ºC and calcined at appropriate temperature to eliminate the surfactants. Interestingly, the size of spherical PS-*b*-PEO aggregates (the number of PS-*b*-PEO molecules in the aggregates) was variable on the basis of the amount of water. Therefore, pore diameter
70 related to the size of the colloidal PS-*b*-PEO template was controllable from large mesopores (30 nm) to macropores (200 nm).

Addition of organic swelling agents is another significant way to expand the pore sizes. The hydrophobic organic species can be
75 solubilized inside the hydrophobic regions of surfactant micelles based on the hydrophobicity-hydrophobicity interactions, leading to the micelle swelling. With cetyltrimethylammonium bromide acting as a structure-directing agent and 1,3,5-trimethylbenzene (TMB) as an auxiliary one, Qiu *et al.* prepared a series of
80 hierarchically porous HKUST-1 with adjustable interconnecting micropores and mesopores by self-assembly of the framework-building blocks in the presence of surfactant micelles.[102] The synthesized mesostructured MOFs possessed a mesopore system with diameters tunable from 3.8 to 31.0 nm that depended on the
85 synthetic conditions. Additionally, the mesoporous walls were constructed by crystalline microporous network containing a 3D system of channels with a pore diameter of 0.82 nm, which was confirmed by the XRD, N_2 sorption, and TEM analysis. The surface area of the MOFs decreased remarkably from 1124 to 579
90 m^2 g^{-1} with the increase of TMB/CTAB molar ratio from 0 to 0.50. However, the enlargement of pore sizes usually implicates the sacrifice of the specific surface area.

2.2.5 Enhancing the crystallization of pore walls
A high degree of crystallinity of the hybrid structures is quite
95 significant for improving the properties and applicability in many fields. The attempt to crystallize the materials through heat treatment always resulted in the collapse of the periodic mesoporous structures and the deterioration of the hybrid frameworks, which could impede the extended applications.[103]
100 Microwave-assisted synthesis has been shown to be a facile and moderate approach in promoting the crystallization of porous materials at a relatively low temperature.[104,105] And so, Ma *et al.* reported the successful preparation of ordered mesoporous hexagonal metal (Ti, Zr, V, and Al) phosphonate materials with
105 microporous crystalline walls by using a microwave-assisted procedure in the presence of the triblock copolymer F127 as a template.[99] The metal phosphonates possessed a hierarchical porous structure with pore sizes of 7.1-7.5 nm for mesopores and 1.3-1.7 nm for micropores, respectively, and were thermally
110 stable up to approximately 450 ºC. The crystalline phase of these phosphonate-based hybrids could be attributable to the corresponding metal phosphonates crystals formed by the extensive coordination of phosphonic claw groups with metal ions rather than tiny titania particles, which was confirmed by the
115 XRD and TEM characterization.

The pivotal factor to obtain well-defined mesoporosity and fine crystallization is to slow down the coordination rates between the metal centers and organic linkers so as to allow the

assembly of nanosized building blocks and surfactant micelles. Acetic acid can chelate many metal ions, such as Cu^{2+}, to form a derivative of metal-acetate bidentate bridging.[106] Namely, the acetic acid could compete with the carboxylate linkers to

5　coordinate with metal ions and influence the deprotonation of the linker as well. Under the synergic effect of both factors, phase segregation was limited thus to fit the liquid-crystal templating mechanism. N_2 adsorption-desorption, TEM and XRD indicated the generation of well-defined mesopore channels within the

10　microporous copper carboxylates, which presented high crystallinity assigned to the HKUST-1. But the mesostructure was of no long-range order.
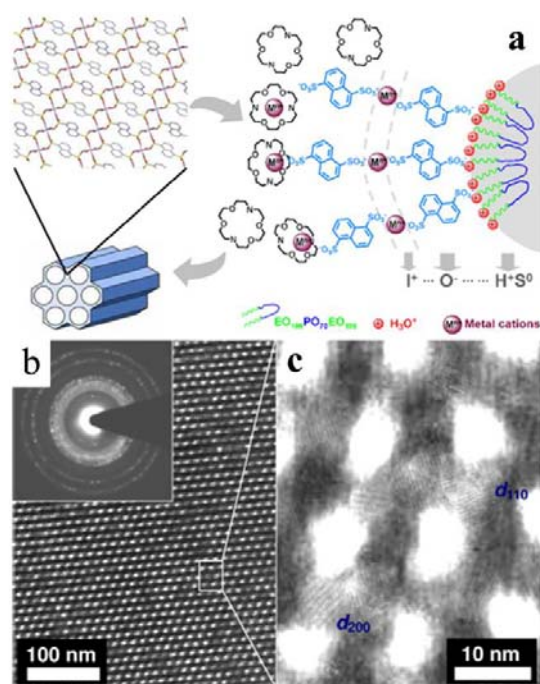
Fig. 4 Schematic model for the formation of mesoporous MOFs, and the
15　coordination numbers in the right figure did not reflect the real situation (a). TEM images and electron diffraction pattern (b, c). Reprinted with permission from ref. 107.

The positively charged surfactants (S^0H^+) and cationic inorganic species (I^+) are assembled together by a combination of
20　electrostatic, hydrogen bonding, and van der Waals interactions (S^0H^+)$\cdots X^-\cdots I^+$　(X^- = Cl^-, NO_3^-, $H_ySO_4^{-2+y}$, *etc.*). If X^- was substituted by disulfonate anions, an analogous mechanism was proposed to be accomplished to form a series of highly ordered mesoporous metal sulfonates.[107] The coordination expansion
25　based on X^-I^+ could form pillared-layered metal disulfonates in the mesoporous wall. The controlled release of metal ions by crown ether 1,10-diaza-18-crown-6 (NC) is necessary to slow down the coordination rate between inorganic and organic species (Fig. 4), and thus finally to retard nucleation kinetics and crystal
30　growth of the MOFs around the micelles. Other common ligands including ethylenediamine, ethylene diamine tetraacetic acid, nitrilotriacetic acid, 2,2'-dipyridyl, and ethylene diamine tetra(methylene phosphonic acid) were also tried to replace crown ether, but no ordered mesopores were observed in the dense
35　crystalline products, and in some cases, impure phases related to the coordination of new added ligands with metal cations also appeared. This was probably because the hydrophobic surface of

NC could effectively isolate the innerly embedded metal cations from the sulfonate anions during the hydrothermal process. This
40　soft-templating assembly route should be generally transferrable to other mesoporous MOFs with appropriate choice of functional groups.

2.3 Morphological design

Well-structured and controllable morphology of porous
45　nanomaterials is of great importance for practical applications. The possibility to fabricate films, spheres, monoliths and so on has been explored. Different morphologies show distinct potentials in various areas such as films in catalysis and separation, spheres in chromatography and drug delivery, and
50　monoliths in optics. Controllable synthesis on both the mesoscale (mesostructure) and macroscale (morphology) is therefore necessary.

Surfactant molecules can selectively adsorb onto the crystallographic planes to dominate the crystallite growth other
55　than performing as onefold templating agents. Thus, by increasing the concentration of surfactant, the shapes of mesoporous MOFs with microporous crystalline walls changed from hexagonal via round to square shaped nanoplates.[108] Various desired morphologies could be obtained by controlling
60　the crystallite growth on confined substrates. The growth of highly crystalline homogeneous MOF thin films was performed on mesoporous silica foam by a layer-by-layer method, and the hierarchically porous hybrid systems combining both micro- and mesoporosity were then available.[109] The preferential orientation
65　of film was along [111], due to the interactions between metal ions and the OH groups on the silica foam surface.

As to PMO-type materials, morphological variation is possible via the EISA methodology.[110] In accordance with this strategy, a great diversity of hybrid inorganic-organic materials with
70　controllable morphologies can be achieved by the combination with the existing techniques including spin-coating and spray-drying and so forth. Ordered mesoporous aluminum phosphonate films with high transparency was prepared through spin-coating of the ethanol-water solution containing methylene diphosphonic
75　acid, aluminum chloride and $EO_nPO_mEO_n$-type triblock copolymer.[98] Careful heating was essential to keep the mesostructure after surfactant removal.

The aerosol-assisted methodology is an effective approach to obtain spherical particles of silica-based and non-silica-based
80　materials, which is based on the sprayed aerosol particles sacrificing and serving as "spherical templates" during the heat treatment process.[111] Spherical aluminum phosphonate particles with uniform mesopores could be fabricated with the assistance of triblock copolymers by temperature-dependent spray-drying
85　(Fig. 5a and b).[112,113] Pore diameter was widely controlled from 6 to 21 nm by changing surfactants and adding organic additives. In order to obtain periodic mesostructures inside the spherical morphology, the evaporation rate of the solvents (ethanol and water) should be moderate. This could allow the residual soluble
90　species infiltrate within the surfactant scaffolds for the construction of resultant hybrid frameworks with sufficient density.[113] With a further increase of the amount of surfactant molecules with expanded cores (PS-*b*-PEO), aluminum phosphonates of fibrous morphology were mixed in the spherical
95　ones at a high spray-drying temperature (230 ºC) due to the high

viscosity of the cloudy precursor solutions (Fig. 5c and d).[101]
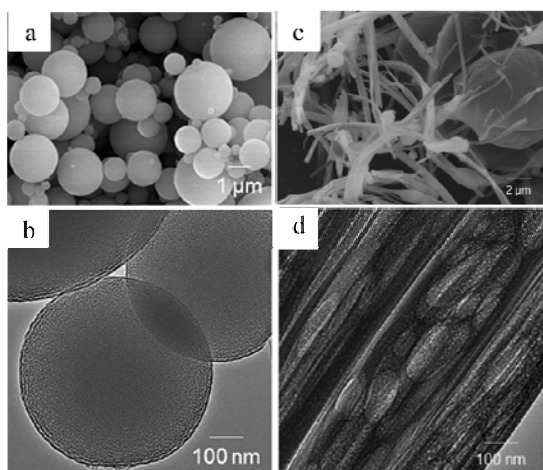
Fig. 5 Porous spherical (a, b) and fibrous (c, d) aluminum phosphonate particles prepared through spray-drying method in the presence of P123 and colloidal PS-b-PEO templates, respectively. Reprinted with permission from ref. 101 and 113.
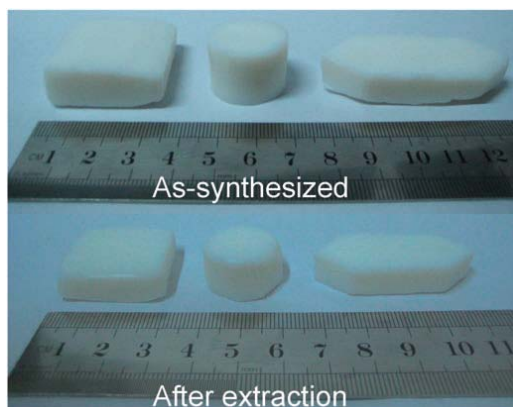
Fig. 6 Photographs of as-synthesized periodic mesoporous titanium phosphonate materials and the final monolithic product after surfactant removal by extraction. Reprinted with permission from ref. 82.

By precisely adjusting the composition of the solutions, spherical titanium phosphonate with an average diameter of 400-500 nm could merely prepared by utilizing a water/ethanol ratio of 3:1.[83] The resulting materials exhibited a hexagonal mesophase in accompany with a BJH pore width of about 2.2 nm and a specific surface area of 606 m^2 g^{-1}. In addition, irregular macrovoids could be observed throughout the hybrid microspheres, which would facilitate mass transport through the microspheres. After experiencing a low-temperature hydrothermal aging, the complete condensation and coordination of titanium and phosphonic acid could result in the generation of a transparent liquid with great viscosity in the presence of oligomer surfactant. The solvent was subsequently evaporated at 50 ºC similar to EISA method, resulting in titanium phosphonate monoliths.[79,82,83] The as-synthesized samples could be molded into various macroscopic morphologies, and valuably, the monolithic shape could be well preserved even after surfactant removal,[82] as shown in Fig. 6. This might potentially fulfill the qualifications for some industrial devices. The organophosphonate groups were homogeneously incorporated in the framework of the periodic mesoporous hybrid solids,

presenting a thermal stability up to approximately 450 ºC.

The controlled synthesis of mesoporous non-siliceous inorganic-organic hybrids includes the adjustment of pore sizes, mesophase symmetry, crystallinity of pore walls and micro-/macroscopic morphologies. Various mature and burgeoning technologies can be employed to attain the desired targets. However, the achievement of well-structured mesophases and high crystalline degree at the same time is still a contradiction. The effective control of mesophase is still challenging, but especially significant in the areas of adsorption, separation, and catalysis. A step further should be meaningful for the broad application prospects.

3 Modification and potential applications

The applications of mesoporous non-siliceous hybrid materials have been widely reported in the past decades, which are mainly based on the well-structured mesoporosity and the instinct of the organic and inorganic units. The hybrid frameworks also demonstrate the capability of post-decoration for improved performances and extended potential applications. Some recent progress is presented as follows.

3.1 Adsorption and separation

As one of the most important potentials of mesoporous hybrids, adsorption has attracted much interest, such as storage of fuel gases (*e.g.*, hydrogen and methane) and greenhouse gas (*e.g.*, carbon dioxide) capture. Selection of the right molecular building blocks can effectively tune the framework connectivity, pore size, and surface area of a MOF, and thereby optimize its hydrogen sorption capacity. Yaghi and co-workers synthesized a series of mesoporous MOFs with ultrahigh surface area, which exhibited large total hydrogen uptake at 77 K.[114] Zhou *et al.* presented a mesoporous PCN-105 presenting hydrogen uptake at 1.0 bar of 1.51 wt % at 77 K and 1.06 wt % at 87 K, respecyively.[115] Generally, the functionality of the organic linkers has little influence on hydrogen sorption, and a large MOF cavity does not make effective contributions to excess hydrogen uptake capacities. Improving the interactions between H_2 and the framework presents a major challenge and bottleneck for MOFs to store hydrogen in a practical manner. An alternative high-density fuel source to hydrogen and gasoline is methane, due to its cleaner and more abundant nature. Walton *et al.* reported that the methane adsorption capacity in micro-/mesoporous UMCM-1 at 298 K was 8.0 mmol g^{-1} at 24.2 bar.[116] Unlike hydrogen, the interactions between methane and the aromatic hybrid framework are strong enough. The safe, cheap and convenient means for methane storage are still in its deficiency. Rigorous research towards robust and available mesoporous or even hierarchical porous hybrid materials for large-scale applications is urgently needed.

The CO_2 amount in the Earth's atmosphere levels up rapidly with the fast development of the industrialization, which has caused the alteration of the temperature of the atmosphere and acidity of the ocean. One feasible option to curtail the rise of the threats is to capture CO_2 from the combustion of fossil fuels. Many amine-functionalized mesoporous siliceous organic-inorganic hybrid materials[117] were proven to be efficient adsorbents for CO_2 capture through the formation of carbamate

species between the solid amine-based adsorbent and the gaseous CO_2 under dry conditions. In recent years, much attention has been focused on mesoporous non-siliceous hybrids for CO_2 capture, due to ultrahigh surface area, adjustable surface chemistry and relatively low-cost.[25,118-120] The CO_2 uptake of the cubic mesoporous titanium phosphonates was approximately 1.0 mmol g^{-1} at 35 °C,[91] which was much higher than some pure silica adsorbents and comparable with some amino-modified mesoporous silicas with similar surface areas.[121] Theoretically, the incorporation of accessible nitrogen-donor groups into the network of porous materials can dramatically influence the gas uptake ability, especially for base carbon oxide.[122] Thus, combined with the superiority of large surface area and high pore volume, the CO_2 uptake capability could be enhanced obviously (about 36.7 wt% at 1 atm and 273 K) when nitrogen-rich organic linkages were intentionally used.[123]

Besides the majority of efforts have been concentrated on the gas adsorption or storage, mesoporous hybrid materials have recently been developed as adsorbents for the removal of heavy metal ions, in which the organic functionalities of these adsorbents serve the formation of complexes with heavy metal ions through acid-base interactions. For instance, the coupling organophosphonic molecules were homogeneously incorporated into the mesoporous walls of the titanium phosphonate materials, and the specific structure of ethylenediamine could chelate metal ions.[79] The adsorption of Cu^{2+}, Pb^{2+}, and Cd^{2+} appeared to follow a Langmuir-type behavior, with the ions being almost quantitatively adsorbed until saturation of the binding sites was reached. The calculated maximum adsorption capacity was 36.49, 29.03, and 26.87 mmol g^{-1} adsorbent for Cu^{2+}, Pb^{2+}, and Cd^{2+}, respectively. Further experiments confirmed that, besides the ethylenediamine groups, many electronegative groups or atoms including -OH, -SH, and N, could contribute to metal ion adsorption. Moreover, competitive adsorption experiments demonstrated that the phosphonate-based adsorbents had an innate selective affinity for the adsorption of one particular ion over the others. A distinct preference of the PMTP-1 adsorbent for the uptake of Cu^{2+} ions, compared with that of Pb^{2+} and Cd^{2+} ions, was observed. This phenomenon was observed in previous ethylenediamine-containing mesoporous silica, which had also a distinct preference for the uptake of Cu^{2+} ions over Ni^{2+} and Zn^{2+} ions.[124] Therefore, it is important from a technical point of view to select suitable coupling molecules with a specific structure and to enlarge the surface area and pore volume of the hybrid materials, and thus to improve the adsorption performance.

The presence of functional groups inside the structure, and the excellent physicochemical properties of the phosphonate-based hybrids including well-ordered pores, large surface areas and pore volume as well as high stability, could be the reason for the improved selectivity. Ma *et al.* firstly tried to use the metal phosphonates as the stationary phase in the open-tubular capillary electrochromatography (OTCEC) separation technique,[99] which combined the efficiency of capillary electrophoresis and the selectivity of high performance liquid chromatography (HPLC). The elution order was benzene < nitrobenzene < naphthalene < anthracene on a crystalline mesoporous titanium phosphonate (EDTMP-Ti) coated capillary, which suggested a hydrophobicity mechanism for the separation of the species (Fig. 7). Noticeably,

by using ordered mesoporous titanium phosphonate materials constructed from the same coupling molecule EDTMP, but with an amorphous framework (PMTP-1),[79] benzene, naphthalene, and anthracene could be well separated, whereas benzene and nitrobenzene could not be completely separated. It was suggested that, besides the hydrophobic interaction, a suitable polarity of the crystalline EDTMP-Ti could be of benefit for the separation of benzene and nitrobenzene. Jiang *et al.* prepared three non-, micro- and mesoporous Cd-MOF isomers, and the mesoMOF was employed as stationary phase for liquid chromatography (LC) separations.[125] The open channel of mesoMOF has a dimension of 1.7×2 nm^2, which could facilitate the incorporation of Rh6G $(1.3 \times 1.6$ nm$^2)$ whereas exhibit size-exclusion of the larger dye Brilliant Blue R-250 $(1.8 \times 2.2$ nm$^2)$. And the microMOF isomer $(0.8 \times 1.5$ nm$^2)$ with smaller pores could not work.
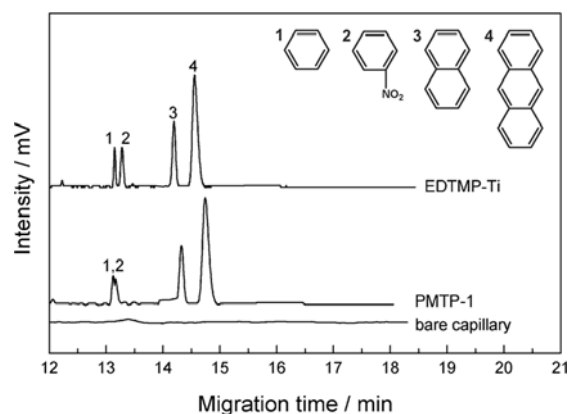

Fig. 7 OTCEC separation of neutral compounds at pH 3.0. PMTP-1 and EDTMP-Ti stand for amorphous[79] and crystalline[99] ordered mesoporous titanium phosphonates, respectively. Reprinted with permission from ref. 99.

The capacity of gas or liquid adsorption/separation is directly related to the surface area, pore volume, pore sizes, and framework composition. Thermal, chemical, and mechanical stability are crucial to the practical applications of mesoporous hybrids. Adjusting pore width through using organic groups with demanded length or proper surfactant molecules can make the adsorption or separation of guests with different dimensions feasible. Engineering pore walls with exquisite functionalities enables further potential of mesoporous hybrid materials in separating some special mixtures that cannot be finished by classical porous inorganic solids, for example, liquid/liquid separation and enantioselective separation.

3.2 Energy conversion and storage

Recently, mesoporous hybrid inorganic-organic materials have been examined in energy conversion applications. Pristine titania is one of the most investigated photocatalysts for environmental remediation and energy storage due to the industrial availability, stability and appropriate band gap. However, pure titania allows only absorption of the UV portion of the solar radiation. As many guest ions could be introduced into the titania framework via phosphonic modification, mesoporous titanium phosphonates were considered to be potential photocatalysts. In general, the homogeneous doping (C, P, and N, *etc.*) of titanium phosphonates network from the bridging molecules and well-structured porosity could increase the photoadsorption efficiency and enhance the

mass transfer. Correspondingly, a noticeable shift of adsorption edge to visible-light region was achieved for titanium phosphonate, in contrast to that of pure titania.[126] Interestingly, the band gap energies could be descended by lowering the pH

5 value of the synthesis system.[45] The shift of the absorption onset toward the lower energy range revealed that the titanium phosphonate materials might make a better use of solar energy. The photocatalytic activity of these materials was enhanced because of the absorption edge shifting to higher wavelengths,

10 except for the sample synthesized at pH = 10.5, which had a small surface area. The extension of the absorption to visible region of titanium-based phosphonate hybrids resulted in an unprecedentedly impressive photoactivity under the simulated solar light illumination. When the porous structure was adjusted

15 properly with a large surface area of more than 1000 m^2 g^{-1}, the photocatalytic activity could be further enhanced due to the presence of more active adsorption sites.
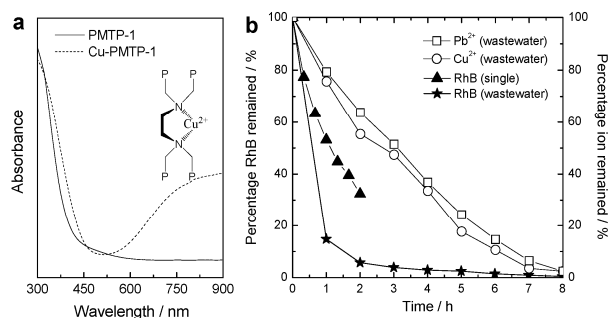
Fig. 8 (a) UV-vis diffuse-reflectance spectra of PMTP-1 before and after
20 Cu^{2+} ion loading; b) one-pot heavy metal ion adsorption in the wastewater treatment as well as RhB photodegradation by using PMTP-1 under simulated solar light irradiation. Reprinted with permission from ref. 79.

Normally, most of the wastewater produced by industrial process and household contain both organic and inorganic
25 contaminants, such as, heavy metal ions and dyes. To cater for the need of the practical applications, a comprehensive catalyst is urgently required.[79] The mixtures of Rhodamine B (RhB), Cu^{2+}, and Pb^{2+} were selected as probes. In the presence of ordered mesoporous titanium phosphonate, the concentration of RhB
30 decreased in the early 2 h and the photodecoloraction rates decreased in the next 6 h until the dyes were completely decomposed. A degradation efficiency of 89.2% was achieved after 100 min of irradiation, which was even higher than the degradation degree for RhB on its own (68.4%) after the same
35 interval. This could be explained by a new broad absorption peak between 600-900 nm caused by the complex of Cu^{2+} on the surface of the hybrid network, giving rise to a better use of visible light. Independently, the concentrations of the metal ions decreased gradually with the reaction time, and nearly 98 % of
40 ions could be removed after 8 h experiment, which signified that the presence of RhB did not prohibit the adsorption process of the heavy metal ions. Both organic and inorganic pollutants could be eliminated under simulated solar light radiation, while the homogeneously coordinated metal ions on the hybrid materials
45 could improve the photocatalytic activity simultaneously (Fig. 8).[79] This inspired us with an alternative method for the preparation of new photocatalysts.
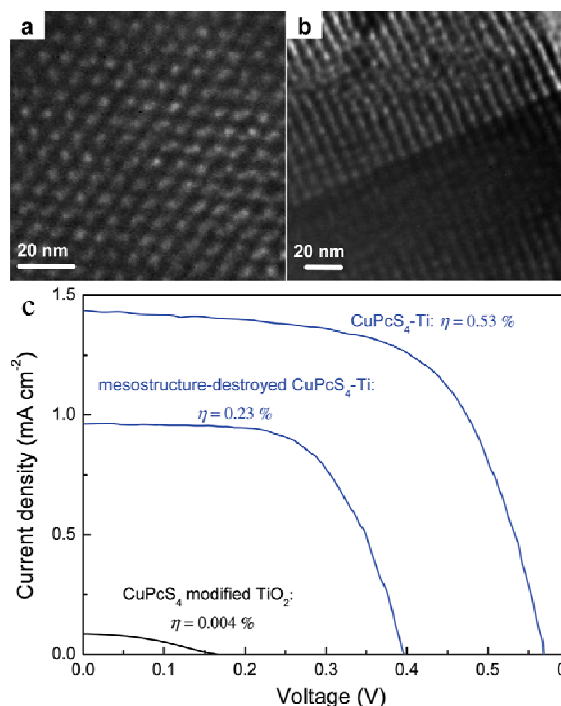
Fig. 9 (a, b) TEM images of hexagonal mesoporous titanium
50 tetrasulfonates (CuPcS$_4$-Ti) with large conjugated hybrid framework and (c) I-V curves of the mesoporous CuPcS$_4$-Ti-based solar cell under simulated sunlight irradiation. Reprinted with permission from ref. 100.

Dye-sensitized solar cells (DSSCs) have been widely investigated since 1991.[127] Up to now, by subtly designing the
55 organic photoactive dye molecules, judiciously choosing the eletrolytes and optimizing the assembling technology, the energy conversion efficiency could be promoted to as high as approximately 15%.[128] However, the costly dyes and complicated fabrication procedure are typically involved, which prohibit their
60 practical potential. On the other hand, traditional preparation for the dye-sensitized electrodes of solar cells is accomplished by the adsorption of dye molecules onto the presynthesized semiconductor electrodes, which usually leads to a very low loading amount of the photosensitive molecules. An alternative
65 strategy for the construction of new DSSCs was proposed by using hybrid metal sulfonate mesoporous materials with large conjugated hybrid framework (Fig. 9).[100] Substituted dye molecules like phthalocyanines with sulfonic groups could be used as the coupling molecules. The one-pot condensation
70 between metal precursors and dyes allowed the molecular-level penetration of large π-aromatic groups into the semiconductor network homogenously, resulting in an unprecedented large loading amount of organic dyes, but without the disadvantages of dye aggregation and electron ill-transmission, because of the
75 isolation of single dye centers by the surrounding semiconductor oligomers. Mesoporous titanium tetrasulfonate materials were then prepared and used in DSSCs to obtain a photoelectric conversion efficiency of 0.53%. More metal phosphonates, sulfonates and carboxylates with large conjugated structures are
80 still expected.

Thus, a functionalized pore system for energy conversion and storage can be derived from either inorganic components or organic bridging groups with fine photosensitivity, and their synergistic effect can further improve the ultimate performance.

So mesoporous hybrid materials have provided a promising platform for solar energy utilization. If the catalytically competent Ir, Ru and Re complexes with functional organic linkers were introduced into the hybrid framework, the final materials could be used to catalyze water oxidation and CO_2 reduction. It is then worthwhile on developing and inventing photosensitive, conductive, or even redox-active porous hybrids for energy conversion and storage in the coming years.

3.3 Heterogeneous catalysis

Heterogeneous catalysis of inorganic porous materials is of great importance for many industrial productions. With the incorporation of well-defined organic moieties into the solid framework, mesoporous hybrid materials are extraordinarily suitable to afford uniform catalytic sites and adjustable porosity for size-, shape-, chemo-, and stereoselective reactions.[129] Also, mesoporous hybrid solid catalysts are simply separated from the reaction systems for recycling. A flake-like tetragonal tinphosphonate with mesoscopic voids, synthesized by using diphosphonic acid as spacers, could be employed as catalyst for the polymerization of styrene to polystyrene in the absence of solvent and for partial oxidation of styrene to phenylacetaldehyde and acetophenone in the presence of various aprotic solvents, and dilute aqueous H_2O_2 acted as an initiator/oxidant.[130] The polymerization could be finished at room temperature within 2 – 3 h reaction time. But the BET surface area was relatively low, only 338 m^2 g^{-1}. By using surfactant as structure directing agent, the surface area of tin phosphonate could be increased to 723 m^2 g^{-1}, accompanied with micropores due to crosslinking of the ligand.[131] This material showed excellent catalytic activity in direct one-pot oxidation of cyclohexanone to adipic acid using molecular oxygen under liquid phase conditions. The tin in the framework activated the molecular oxygen, helping to form the cyclic six-membered transition state,[132] which further rearranged into a cyclic ester.

Asymmetric catalysis is of vital significance for the medicinal and pharmic application potential, and the core is the invention of chiral catalysts. Surface modification seems to generate chirality facilely,[133] but this route tends to reduce the pore sizes and hence negatively impacts the catalytic activity owing to the inhibition of mass diffusion through the channels. By using chiral Mn-Salen-derived linkages, a family of chiral carboxylate-based MOFs with tuneable open channels were rationally designed and synthesized.[134] These isoreticular chiral MOFs were demonstrated to be highly active in catalyzing enantioselective alkene epoxidation reactions. The epoxidation reaction rates were strongly dependent on the pore sizes, indicating that larger channel dimensions could increase the reaction rate by facilitating the diffusion of reactant and product molecules. Furthermore, different metal centers acted as primary catalytic sites, which could be integrated into the organic linkers, being applied to catalyze various reactions to allow multiple steps manipulations of organic substrates with a single solid.[135]

Mesoporous non-siliceous solid acids have recently been developed for the use in acid-catalyzed organic reactions. Mesostructured zirconium phosphonate, possessing a specific surface area of 702 m^2 g^{-1} and a uniform pore size of 3.6 nm, was synthesized with the assistance of CTAB, using 1-hydroxyethylidene-1,1-diphosphonic acid (HEDP) as coupling molecule.[136] XPS, FT-IR and NMP confirmed the existence of defective P-OH, and the resulted ion exchange capacity of the hybrid was 1.65 mmol g^{-1}. The resultant hydroxyethylidene-bridged mesoporous zirconium phosphonate could serve as acid catalyst for the synthesis of methyl-2,3-O-isopropylidene-β-D-ribofuranoside from D-ribose, exhibiting high catalytic activity with rapid reaction rate, which were comparable to the catalytic performance of liquid acid HCl or commercial ion-exchange resin. Acid content and strength are the two key elements to determine catalytic activity and efficiency. To enhance the acidity, a further functionalization was effective. The specific alkyl hydroxyl structure of the coupling molecule HEDP makes its sulfation possible and facile.[82] The -SO_3H groups were introduced by $ClSO_3H$ treatment to form relatively stable hydrosulfated esters. Approximately 2.69 and 3.93 mmol g^{-1} of H^+ were assigned to the grafted sulfonic groups and to the defective P-OH from the hybrid framework, respectively. The acid strength revealed a Hammett indicator of $H_0 < -11.35$, indicative of a strong solid acid. For example, the sulphated materials could be used in the esterification of oleic acid and methanol under ambient temperature and pressure, giving a much higher conversion (87.3%) than the unfunctionalized materials (4.9 %). Based on acid-base reactions, the P-OH in the phosphonic precursors could be effectively protected to increase the defective acid amount by the addition of a series of alkyl amine.[137] The highest H^+ exchange capacities could be confirmed as 5.51 – 5.80 mmol g^{-1}, which led to high yields of 48.7 % for methyl-2,3-O-isopropylidene-β-D-ribofuranoside.

CO_2 is the main greenhouse gas. Also as an abundant, non-toxic, and renewable C1 building block, the chemical conversion of CO_2 is being increasingly considered as a means of effective sequestration. Cyclic carbonates derived from the coupling reactions of CO_2 and epoxides are promising chemicals since they show potential as electrolytes in lithium-ion batteries, raw materials in for polycarbonates and polar aprotic solvents.[138] Song *et al.* reported the coupling reaction of CO_2 with propylene oxide to produce propylene carbonate catalysed by MOF-5 in the presence of quaternary ammonium salts.[139] The synergetic effect between MOF-5 and quaternary ammonium salts had excellent effect in promoting the reaction. The cycloaddition of CO_2 has known to be catalyzed by basicity in a heterogeneous catalyst and promoted by the Lewis acidic sites.[140] Carboxylate-based MOFs is usually known for the Lewis acidity after the removal guest molecules. The incorporation of basic amino groups into UIO-66 to form UIO-66-NH_2 could lead to the enhanced catalytic performance.[141] The resultant samples showed nearly 100 % selectively to carbonate in chlorobenzene under relatively mild reaction conditions (2.0 MPa, 373 K). Bifunctional heterogeneous hybrid catalysts containing moderate Lewis acidic and basic sites are preferred in the cycloaddition reactions. Whereas the activation and ring-opening of epoxides are the most difficult steps in the reaction as they had the largest activation energy.[142] However, this is usually accomplished by commercially available homogeneous co-catalysts including quaternary ammonium salts and halides. To develop a heterogeneous catalyst with desired functionalities through pre- or post-modification for synthesizing cyclic carbonates at mild conditions remains a challenge.

Carbon monoxide (CO) is harmful to human health and

environment even at a very low concentration. For the control of the toxic emission, catalytic oxidation of CO is an efficient way. Although novel metals have presented high activity, the high cost and limited availability discourage their extensive applications. It is commonly accepted that a high dispersion of active components on the supports can contribute toward improving the catalytic oxidation ability of different catalysts.[143] Thereafter, homogeneous coordination of metal ions (*e.g.*, Cu^{2+}) on the hybrid surface, followed by low-temperature calcination, which could transform the chelated ions to corresponding metal oxides with high dispersion.[83] More importantly, the density and the distribution of the surface organic functional groups could be tuned, allowing for an indirect adjustment of the dispersion of the Cu^{2+} complex and the final CuO layer. XRD, N_2-sorption and H_2-TPR indicated the successful high adhesion. The CO catalytic activity of the synthesized catalyst was higher than those of materials with the same CuO content but prepared via other conventional methods.

Catalytic reactions are typically surface processes where exist substantial host-guest interactions. So, scrumptious changing the surface composition of the porous hybrid will arouse multitudinous catalytic activities, which can be accomplished by varying organic linkages and post-functionalization. The post-functionalization is typically based on different organic motifs integrated in the hybrid framework. Esterification could be performed by using the bridging groups containing hydroxyls; nitration and sulfonation were feasible by means of hybriding with aromatic bridging group; acylation and oxidation were possible in the presence of amino groups in the framework. Ultimately, hydrophilicity/hydrophobicity, acidity/alkalinity, and even chirality are resulted in the hybrid frameworks.

3.4 Biomaterials

The capacity of mesoporous inorganic-organic hybrid materials to be designed with special functionality together with meaningful porosity and biocompatibility not only makes them stand out from traditional porous materials, but also promises great potential to be a new category of biomaterials. However, the special area has not been explored as broadly as adsorption/separation and catalysis applications. Immobilization of enzymes on the proper solid supports can improve enzyme stability, facilitate separation and recycling, and maintain the catalytic activity and selectivity as well.[144] Classical mesoporous silicas usually suffer from the easy leaching of immobilized enzyme molecules due to the lack of interactions between enzymes and host materials, which results in the loss of catalytic activity upon multiple uses reversely. With organic components in the hybrid materials, microperoxidase-11 (MP-11) could be successfully immobilized in mesoporous MOFs containing nanoscopic cages of around 4.0 nm under the drive of host-guest hydrophobic interactions.[145] The corresponding loading amount could reach to 19.1 μmol g^{-1}. Accordingly, as compared with the mesoporous silica counterpart, the resulting enzyme-loaded MOFs exhibited superior enzymatic catalysis performances and reusability for polyphenol oxidation in the presence of hydrogen peroxide.

Férey *et al.* tested the abilities of MIL-100(Cr) and MIL-101(Cr) for delivery of Ibuprofen, showing remarkable adsorption with 0.347 g g^{-1} and 1.376 g g^{-1}, respectively.[146] And the complete release of Ibuprofen was achieved for MIL-100(Cr) and MIL-101(Cr) after 3 and 6 days, respectively. Compared with MCM-41, MIL-101(Cr) demonstrated four times higher loading capacity and much longer releasing time (2 days for MCM-41), which was probably due to the stronger interaction between Ibuprofen and the MIL-101(Cr) framework (π-π and acid-base interactions). But chromium is toxic, prohibiting the further clinical applications. The biocompatible nanoscale Fe-MIL-100 along with microporous iron(III) carboxylate were prepared by Férey *et al.* for drug delivery and imaging to reconcile the cytotoxicity and high drug loading capacity.[147] The low toxicity was confirmed by the reversible weight increase and return to normality after injection in one to three months as well as the absence of immune or inflammatory reactions. The antitumoural drug busulfan (Bu) could be loaded into Fe-MIL-100, and the same activity was obtained for the entrapped Bu as free Bu due to entrapped Bu in its molecular form within the pores.

Controlled drug delivery and release technology offers numerous advantages in comparison with conventional dosage forms including improved efficacy, reduced toxicity, and improved patient compliance and convenience.[148] This process mainly depends on the variations of pH, light, redox potential and temperature. The designed delivery systems of "molecular lock" are able to selectively release the entrapped guests. pH-sensitive mesoporous zirconium phosphonate was thus prepared through a surfactant-assisted procedure by using 1,4-bis(phosphomethyl)piperazine as the bridging groups.[149] The pH-sensitivity was derived from the reversible protonation under acidic conditions and deprotonation under weakly basic medium of piperazine moieties integrated in the framework under different pH conditions. This endowed mesoporous phosphonate with reversible cationic-neutral surface properties. The negatively charged PDS (dinuclear cobalt phthalocyanine ammonium sulfonate, a photosensitizer of sulfonated phthalocyanine for photodynamic therapy of tumors) could then be adsorbed or released through strong electrostatic interaction according to the pH condition. The equilibrium capacity for PDS reached as high as near 300 mg g^{-1}. Valuably, extremely little PDS was released under simulated acidic environment of stomach (pH = 1.2) within 48 h while a sustained release in the simulated environmental pH value of the intestine (pH = 7.5).

So far, detection and medication of organism diseases are two consecutive and inseparable processes in clinical diagnostics and treatment, but their academic studies are often isolated from each other. It is still challenging and significant to design a "diagnospy" carrier that combines the functions of biomolecule quantitative detection and bioresponsive drug controlled release. A smart system has recently intentionally designed on the basis of hybrid phosphonate-TiO_2 mesoporous nanostructures capped with fluorescein labeled oligonucleotides, which could realize simultaneous and highly-efficient biomolecule sensing and controlled drug release (Fig. 10).[150] The incorporation of phosphonate could shift the absorption edge of titania to visible light range and introduce positively charged amino groups to interact with negatively charged fluorescein labelled oligonucleotides, resulting in the closing of the mesopores and the fluorescence quenching of fluorescein at the same time. The further addition of complementary single DNA strands or protein

target led to the displacement of the capped DNA due to hybridization or protein-aptamer reactions. Correspondingly, the pores were opened causing the release of entrapped drugs as well as the restoration of dye fluorescence. This study provides a novel perception to utilize non-siliceous hybrid materials as the supports in sensing and control release applications.
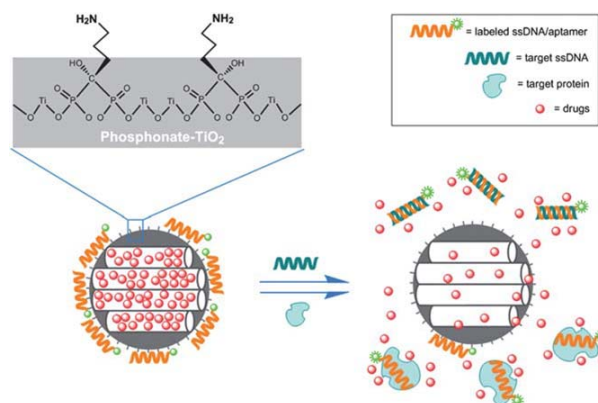
Fig. 10 Schematic illustration of bioresponsive detection and drug controlled release system based on phosphonate-TiO$_2$ hybrid material. Reprinted with permission from ref. 150

4 Summary and perspective

Mesoporous metal carboxylates, phosphonates and sulfonates as the three most fascinating members of non-siliceous hybrids with alternative inorganic-organic frameworks have attracted great research interest in the past decades due to their outstanding physicochemical properties. In order to improve the accessibility of the pores, template-free methodology via enlarging the organic linkages is proved to be facile and effective but restricted. Soft-templating approach has been realized to synthesize mesoporous hybrids with uniform pore width, high surface area, and even hierarchical porosity. The control over the mesophase symmetry, the pore sizes, and the crystallinity of pore walls is relevant to the structure of surfactant molecules and the synthesis method. Morphological adjustment through a variety of fabrication techniques is feasible, which endows them capability in diverse production fields. The synthesized mesoporous non-silica-based hybrid materials could be utilized as efficient host solids for the adsorption and separation of gas, liquid, heavy metal ions, as well as organic constitutes. They were also useful for eco-friendly photocatalysis and solar cells under simulated solar light irradiation, and biomaterials for enzymatic engineering, drug delivery, and medical diagnosis. Further functionalization of the mesoporous hybrids could make them oxidation and acid catalysts, both with impressive performances in the areas of sustainable energy and environment.

In comparison to the counterparts of phosphonates and carboxylates, reports in regard to mesoporous metal sulfonates are relatively scarce. This is mainly resulted from the weaker combination between metal linkers and organosulfonic groups, which leads to a less robust framework. However, besides applications in adsorption/separation and photoelectrochemistry, the weaker ligating nature of sulfonic bridging units predisposes the network to certain degree of flexibility, namely dynamics material. Correspondingly, the resultant materials can be used to selectively adsorb and detect metal ions and small molecules. It can also be envisioned the reversible insertion/desertion of Li$^+$ and protons through the pores and elastic network. Although this aspect is not extensively studied, the intrinsic porosity within the electrically conductive hybrid materials is remain largely unknown but is worthy of research efforts.

The exploration of synthetic methodologies and extended applications of mesoporous non-siliceous hybrid materials remains promising and valuable. Due to the complexity of the interactions between organic groups and metallic centers, the achievement of intentional control over the pore size, pore channel regularity and mesophase is still a challenge. The practical value of mesoporous non-siliceous hybrids is limited by their relatively poor thermal and hydrothermal stabilities as compared with those of silica-based materials. And obtaining a mesoporous structure of crystalline pore walls is expected to be a solution. Mesoporous hybrids demonstrate the combined properties of inorganic units and organic moieties. Thus, judicious selection of metal precursors and design of organic bridging molecules (phosphonic, carboxylic and sulfonic acids) and related derivatives through organic synthesis can extend their applications in multiple areas, such as proton conduction, fuel cells, photoeletricity, and biosensing.

Acknowledgements

Notes and references

^{a} Key Laboratory of Advanced Energy Materials Chemistry (Ministry of Education), Collaborative Innovation Center of Chemical Science and Engineering (Tianjin), College of Chemistry, Nankai University, Tianjin 300071, China. E-mail: zyyuan@nankai.edu.cn.
^{b} School of Chemical Engineering and Technology, Hebei University of Technology, Tianjin 300130, China.

1　P. Yang, D. Zhao, D. I. Margolese, B. F. Chmelka and G. D. Stucky, *Nature*, 1998, **396**, 152-155.
2　B. T. Holland, C. F. Blanford and A. Stein, *Science*, 1998, 281, 538-540.
3　L. Huang, Z. Wang, J. Sun, L. Miao, Q. Li, Y. Yan and D. Zhao, *J. Am. Chem. Soc.*, 2000, **122**, 3530-3531.
4　T. Wakihara, S. Yamakita, K. Lezumi and T. Okubo, *J. Am.Chem. Soc.*, 2003, **125**, 12388-12389.
5　M. E. Davis, *Nature*, 2002, **417**, 813-821.
6　M. Eddaoudi, J. Kim, N. Rosi, D. Vodak, J. Wachter, M. O'Keeffe and O. M. Yaghi, *Science*, 2002, **295**, 469-472.
7　C. H. Tung, L. Z. Wu, Z. Y. Yuan and N. Su, *J. Am. Chem. Soc.*, 1998, **120**, 11594-11602.
8　M. B. Park, Y. Lee, A. M. Zhang, F. S. Xiao, C. P. Nicholas, G. J. Lewis and S. B. Hong, *J. Am. Chem. Soc.*, 2013, **135**, 2248-2255.
9　T. E. Gier, X. Bu, P. Feng and G. D. Stucky, *Nature*, 1998, **395**, 154-157.
10　X. Bu, P. Feng and G. D. Stucky, *Chem. Mater.*, 1999, **11**, 3423-3424.
11　T. D. Tang, L. Zhang, W. Q. Fu, Y. L. Ma, J. Xu, J. Jiang, G. Y. Fang and F. S. Xiao, *J. Am. Chem. Soc.*, 2013, **135**, 11437-11440.
12　C. T. Kresge, M. E. Leonowicz, W. J. Roth, J. C. Vartuli and J. S. Beck, *Nature*, 1992, **359**, 710-712.
13　D. Zhao, Q. Huo, J. Feng, B. F. Chmelka and G. D. Stucky, *J. Am. Chem. Soc.*, 1998, **120**, 6024-6036.

14 S. Che, Z. Liu, T. Ohsuna, K. Sakamoto, O. Terasaki and T. Tatsumi, *Nature*, 2004, **429**, 281-284.

15 J. S. Beck, J. C. Vartuli, W. J. Roth, M. E. Leonowicz, C. T. Kresge, K. D. Schmitt, C. T. W. Chu, D. H. Olson, E. W. Sheppard, S. B. McCullen, J. B. Higgins and J. L. Schlenker, *J. Am. Chem. Soc.*, 1992, **114**, 10834-10843.

16 D. Zhao, J. Feng, Q. Huo, N. Melosh, G. H. Fredrickson, B. F. Chmelka and G. D. Stucky, *Science*, 1998, **279**, 548-552.

17 T. W. Kim, F. Kleitz, B. Paul and R. Ryoo, *J. Am. Chem. Soc.*, 2005, **127**, 7601-7610.

18 M. Kruk and L. Cao, *Langmuir*, 2007, **23**, 7247-7254.

19 S. Inagaki, S. Guan, Y. Fukushima, T. Ohsuna, O. Terasaki, *J. Am. Chem. Soc.*, 1999, **121**, 9611-9614.

20 M. P. Kapoor, Q. Yang, S. Inagaki, *J. Am. Chem. Soc.*, 2002, **124**, 15176 -15177.

21 Y. D. Xia, Z. X. Yang and R. Mokaya, *Chem. Mater.*, 2006, **18**, 1141-1148.

22 J. Perles, N. Snejko, M. Iglesias and M. Ángeles Monge, *J. Mater. Chem.*, 2009, **19**, 6504-6511.

23 H. Furukawa, K. E. Cordova, M. O'Keefe and O. M. Yaghi, *Science*, 2013, **341**, 974-986.

24 W. J. Hunks and G. A. Ozin, *J. Mater. Chem.*, 2005, **15**, 3716-3724.

25 T. Y. Ma and Z. Y. Yuan, *ChemSusChem*, 2011, **4**, 1047-1419.

26 O. R. Evans, H. L. Ngo and W. B. Lin, *J. Am. Chem. Soc.*, 2001, **123**, 10395-10396.

27 W. N. Xuan, C. F. Zhu, Y. Liu and Y. Cui, *Chem. Soc. Rev.*, 2012, **41**, 1677–1695.

28 Q. R. Fang, T. A. Makal, M. D. Young and H. C. Zhou, *Comment. Inorg. Chem.*, 2010, **31**, 165–195.

29 L. F. Song, J. Zhang, L. X. Sun, F. Xu, F. Li, H. Z. Zhang, X. L. Si, C. L. Jiao, Z. B. Li, S. Liu, Y. L. Liu, H. Y. Zhou, D. L. Sun, Y. Du, Z. Cao and Z. Gabelica, *Energy Environ. Sci.*, 2012, **5**, 7508–7520.

30 T. Kimura, *J. Nanosci. Nanotechnol.*, 2013, **13**, 2461–2470.

31 G. Alberti, U. Costantino, F. Marmottini, R. Vivani and P. Zapelli, *Microp. Mesop. Mater.*, 1998, **21**, 297-304.

32 G. Alberti, R. Vivani, F. Marmottini and P. Zappelli, *J. Porous Mater.*, 1998, **5**, 205-220.

33 A. Clearfield, *Chem. Mater.*, 1998, **10**, 2801-2810.

34 S. Konar, J. Zon, A. V. Prosvirin, K. R. Dunbar and A. Clearfield, *Inorg. Chem.*, 2007, **26**, 5229-5236.

35 George K. H. Shimizu, R. Vaidhyanathan and J. M. Taylor, *Chem. Soc. Rev.*, 2009, **38**, 1430-1449.

36 F. Gándara, A. Garca-Corteís, C. Cascales, B. Gómez-Lor, E. Gutiérrez-Puebla, M. Iglesias, A. Monge and N. Snejko, *Inorg. Chem.*, 2007, **46**, 3475-3484.

37 D. J. Hoffart, S. A. Dalrymple and G. K. H. Shimizu, *Inorg. Chem.*, 2005, **44**, 8868-8875.

38 L. Ma, J. M. Falkowski, C. Abney and W. Lin, *Nature Chem.*, 2010, **2**, 838-846.

39 O. M. Yaghi, H. Li, C. Davis, D. Richardson and T. L. Groy, *Acc. Chem. Res.*, 1998, **31**, 474-484.

40 X. S. Wang, S. Q. Ma, D. F. Sun, S. Parkin and H. C. Zhou, *J. Am. Chem. Soc.*, 2006, **128**, 16474-16475.

41 Y. Yan, S. H. Yang, A. J. Blake, W. Lewis, E. Poirier, S. A. Barnett, N. R. Champness and M. Schröder, *Chem. Commun.*, 2011, **47**, 9995-9997.

42 H. Deng, S. Grunder, K. E. Cordova, C. Valente, H. Furukawa, M. Hmadeh, F. Gándara, A. C. Whalley, Z. Liu, S. Asahina, H. Kazumori, M. O'Keeffe, O. Terasaki, J. F. Stoddart and O. M. Yaghi, *Science*, 2012, **336**, 1018-1023.

43 M. Vasylyev, E. J. Wachtel, R. Popovitz-Biro and R. Neumann, *Chem. Eur. J.*, 2006, **12**, 3507-3514.

44 M. Vasylyev and R. Neumann, *Chem. Mater.*, 2006, **18**, 2781-2783.

45 T. Y. Ma, X. J. Zhang and Z. Y. Yuan, *Micropor. Mesopor. Mater.*, 2009, **123**, 234-242.

46 P. Schmidt-Winkel, W. W. Lukens, D. Y. Zhao, P. D. Yang, B. F. Chmelka and G. D. Stucky, *J. Am. Chem. Soc.*, 1999, **121**, 254-255.

47 X. J. Zhang, T. Y. Ma and Z. Y. Yuan, *Eur. J. Inorg. Chem.*, 2008, 2721-2726.

48 X. Y. Yang, A. Léonard, A. Lemaire, G. Tian and B. L. Su, *Chem. Commun.*, 2011, **47**, 2763-2786.

49 Z. Y. Yuan and B. L. Su, *J. Mater. Chem.*, 2006, **16**, 663-677.

50 T .Y. Ma, X. J. Zhang and Z. Y. Yuan, *J. Phys. Chem. C.*, 2009, **113**, 12854-12862.

51 C. Liu, T. Li, N. L. Rosi, *J. Am. Chem. Soc.*, 2012, **134**, 18886-18888.

52 S. Yang, X. Lin, W. Lewis, M. Suyetin, E. Bichoutskaia, J. E. Parker, C. C. Tang, D. R. Allan, P. J. Rizkallah, P. Hubberstey, N. R. Champness, K. M. Thomas, A. J. Blake and M. Schröder, *Nat. Mater.*, 2012, **11**, 710-716.

53 Y. F. Yue, Z. A. Qiao, P. F. Fulvio, A. J. Binder, C. C. Tian, J. H. Chen, K. M. Nelson, X. Zhu and S. Dai, *J. Am. Chem. Soc.*, 2013, **135**, 9572-9575.

54 T. Tsuruoka, S. Furukawa, Y. Takashima, K. Yoshida, S. Isoda and S. Kitagawa, *Angew. Chem. Int. Ed.*, 2009, **48**, 4739-4743.

55 A. R. Hirst, B. Escuder, J. F. Miravet and D. K. Smith, *Angew. Chem. Int. Ed.*, 2008, **47**, 8002-8018.

56 Q. Wei and S. L. James, *Chem. Commun.*, 2005, **41**, 1555-1556.

57 Y. R. Liu, L. He, J. Zhang, X. Wang and C. Y. Su, *Chem. Mater.*, 2009, **21**, 557-563.

58 L. Li, S. L. Xiang, S. Q. Cao, J. Y. Zhang, G. F. Ouyang, L. P. Chen and C.-Y. Su, *Nat. Commun.*, 2013, **4**, DOI: 10.1038/ncomms2757.

59 D. Zacher, R. Schmid, C. Woll and R. A. Fischer, *Angew. Chem. Int. Ed.*, 2011, **50**, 176-199.

60 J. Cravillon, C. A. Schröder, R. Nayuk, J. Gummel and M. Wiebcke, *Angew. Chem. Int. Ed.*, 2011, **50**, 8067-8071.

61 S. Cao, G. Gody, W. Zhao, S. Perrier, X. Y. Peng, C. Ducati, D. Y. Zhao and A. K. Cheetham, *Chem. Sci.*, 2013, **4**, 3573–3577.

62 W. Li and D. Y. Zhao, *Chem. Commun.*, 2013, **49**, 943-946.

63 T. Y. Ma, L. Liu and Z. Y. Yuan, *Chem. Soc. Rev.*, 2013, **42**, 3977-4003.

64 A. Fischereder, M. L. Martinez-Ricci, A. Wolosiuk, W. Haas, F. Hofer, G. Trimmel and G. J. A. A. Soler-Illia, *Chem. Mater.*, 2012, **24**, 1837-1845.

65 P. Yang, D. Zhao, D. I. Margolese, B. F. Chmelka and G. D. Stucky, *Chem. Mater.*, 1999, **11**, 2813-2826.

66 J. S. Yu, S. Kang, S. B. Yoon and G. Chai, *J. Am. Chem. Soc.*, 2002, **124**, 9382-9383.

67 T. F. Baumann and J. H. Satcher, *Chem. Mater.*, 2003, **15**, 3745-3747.

68 Q. D. Nghiem and D. P. Kim, *Chem. Mater.*, 2008, **20**, 3735-3739.

69 B. Z. Tian, X. Y. Liu, B. Tu, C. Yu, J. Fan, L. M. Wang, S. H. Xie, G. D. Stucky and D. Y. Zhao, *Nat. Mater.*, 2003, **2**, 159-163.

70 S. A. Davis, M. Breulmann, K. H. Rhodes, B. Zhang and S. Mann, *Chem. Mater.*, 2001, **13**, 3218-3226.

71 X. Roy, L. K. Thompson, N. Coombs and M. J. MacLachlan, *Angew. Chem. Int. Ed.*, 2008, **47**, 511-514.

72 Y. T. Li, D. J. Zhang, Y. N. Guo, B. Y. Guan, D. H. Tang, Y. L. Liu and Q. S. Huo, *Chem. Commun.*, 2011, **47**, 7809-7811.

73 T. Kimura, *Chem. Mater.*, 2003, **15**, 3742-3744.

74 T. Kimura, *Chem. Mater.*, 2005, **17**, 337-344.

75 T. Kimura, *Chem. Mater.*, 2005, **17**, 5521-5528.

76 J. El Haskouri, C. Guillem, J. Latorre, A. Beltrán, D. Beltrán, P. Amorós, *Chem. Mater.*, 2004, **16**, 4359-4372.

77 J. El Haskouri, C. Guillem, J. Latorre, A. Beltrán, D. Beltrán, P. Amorós, *Eur. J. Inorg. Chem.*, 2004, **9**, 1804-1807.

78 S. Cabrera, J. El Haskouri, C. Guillem, J. Latorre, A. Beltrán, D. Beltrán, M. D. Marcos, P. Amorós, *Solid State Sci.*, 2000, **2**, 405-420.

79 T. Y. Ma, X. Z. Lin and Z. Y. Yuan, *J. Mater. Chem.*, 2010, **20**, 7406-7415.

80 G. J. de A. A. Soler-Illia and C. Sanchez, *New J. Chem.*, 2000, **24**, 493-499.

81 G. J. de A. A. Soler-Illia, E. Scolan, A. Louis, P. -A. Albouy and C. Sanchez, *New J. Chem.*, 2001, **25**, 156-165.

82 T. Y. Ma and Z. Y. Yuan, *Chem. Commun.*, 2010, **46**, 2325-2327.

83 T. Y. Ma and Z. Y. Yuan, *Dalton Trans.*, 2010, **39**, 9570-9578.

84 Y. J. Zhao, J. L. Zhang, B. X. Han, J. L. Song, J. S. Li and Q. Wang, *Angew. Chem., Int. Ed.*, 2011, **50**, 636-639.

85 J. H. Liu, S. Q. Cheng, J. L. Zhang, X. Y. Feng, X. G. Fu and B. X. Han, *Angew. Chem. Int. Ed.*, 2007, **46**, 3313-3315.

86 D. Y. Zhao, Q. S. Huo, J. L. Feng, B. F. Chmelka and G. D. Stucky, *J. Am. Chem. Soc.*, 1998, **120**, 6024-6036.

87 K. W. Gallis, C. C. Landry, *Chem. Mater.*, 1997, **9**, 2035-2038.

88 W. J. Kim, J. C. Yoo and D. T. Hayhurst, *Micro. Meso. Mater.*, 2001, **49**, 125-137.

89 Q. S. Huo, D. I. Margolese and G. D. Stucky, *Chem. Mater.*, 1996, **8**, 1147-1160.

90 J. C. Vartuli, K. D. Schmitt, C. T. Kresge, W. J. Roth, M. E. Leonowicz, S. B. McCullen, S. D. Hellring, J. S. Beck, J. L. Schlenker, D. H. Olson and E. W. Sheppard, *Chem. Mater.*, 1994, **6**, 2317-2326.

91 T. Y. Ma, X. Z. Lin and Z. Y. Yuan, *Chem. Eur. J.*, 2010, **16**, 8487-8494.

92 T. Kimura, D. Nakashima and N. Miyamoto, *Chem. Lett.*, 2009, **38**, 916-917.

93 D. Zhao, Q. Huo, J. Feng, J. Kim, Y. Han and G. D. Stucky, *Chem. Mater.*, 1999, **11**, 2668-2672.

94 Y. H. Deng, J. Wei, Z. K. Sun and D. Y. Zhao, *Chem. Soc. Rev.*, 2013, **42**, 4054-4070.

95 B. C. Garcia, M. Kamperman, R. Ulrich, A. Jain, S. M. Gruner and U. Wiesner, *Chem. Mater.*, 2009, **21**, 5397-5405.

96 S. A. El-Safty, F. Mizukami and T. Hanaoka, *J. Phys. Chem. B*, 2005, **109**, 9255-9264.

97 S. A. El-Safty, T. Hanaoka and F. Mizukami, *Chem. Mater.*, 2005, **17**, 3137-3145.

98 T. Kimura and K. Kato, *New J. Chem.*, 2007, **31**, 1488-1492.

99 T. Y. Ma, H. Li, A. N. Tang and Z. Y. Yuan, *Small*, 2011, **4**, 1407-1419.

100 T. Y. Ma, Y. S. Wei, T. Z. Ren, L. Liu, Q. Guo and Z. Y. Yuan, *ACS Appl. Mater. Interf.*, 2010, **2**, 3563-3571.

101 T. Kimura and Y. Yamauchi, *Chem. Asian J.*, 2013, 8, 160-167. T. Kimura and Y. Yamauchi, *Langmuir*, 2012, **28**, 12901-12908.

102 L. -G. Qiu, T. Xu, Z. -Q. Li, W. Wang, Y. Wu, X. Jiang, X. -Y. Tian and L. -D. Zhang, *Angew. Chem.*, 2008, **120**, 9629-9633.

103 H. Shibata, T. Ogura, T. Mukai, T. Ohkubo, H. Sakai, M. Abe, *J. Am. Chem. Soc.*, 2005, **127**, 16396-16397.

104 H. Y. Chen, H. X. Xi, X. Y. Cai and Y. Qian, *Micropor. Mesopor. Mater.*, 2009, **118**, 396-402.

105 Y. J. Wu, X. Q. Ren and J. Wang, *Micropor. Mesopor. Mater.*, 2008, **116**, 386-393.

106 M. -H. Pham, G. -T. Vuong, F. -G. Fontaine and T. -O. Do, *Cryst. Growth Des.*, 2012, **12**, 1008-1013.

107 T. Y. Ma, H. Li, Q. F. Deng, L. Liu, T. Z. Ren and Z. Y. Yuan, *Chem. Mater.*, 2012, **24**, 2253-2255.

108 L. Peng, J. L. Zhang, J. S. Li, B. X. Han, Z. M. Xue and G. Y. Yang, *Chem. Commun.*, 2011, **47**, 7809-7811.

109 O. Shekhah, L. L. Fu, R. Sougrat, Y. Belmabkhout, A. J. Cairns, E. P. Giannelis and M. Eddaoudi, *Chem. Commun.*, 2012, **48**, 11434-11436.

110 H. Fan, Y. Lu, S. T. Reed, T. Baer, R. Schunk, V. Perez-Luna, G. P. López and C. J. Brinker, *Nature*, 2000, **405**, 56-60.

111 P. Z. Araujo, V. Luca, P. B. Bozzano, H. L. Bianchi, G. J. de Ávila Arturo Soler-Illia and M. A. Blesa, *ACS Appl. Mater. Interf.*, 2010, **2**, 1663-673.

112 T. Kimura, K. Kato and Y. Yamauchi, *Chem. Commun.*, 2009, 4938-4940.

113 T. Kimura and Y. Yamauchi, *Chem. Asian J.*, 2013, **8**, 160-167.

114 H. Furukawa, N. Ko, Y. B. Go, N. Aratani, S. B. Choi, E. Choi, A. Özgür Yazaydin, R. Q. Snurr, M. O'Keeffe, J. K. and O. M. Yaghi, *Science*, 2010, **329**, 424-428.

115 Q. R. Fang, D. Q. Yuan, J. Sculley, W. G. Lu and H. C. Zhou, *Chem. Commun.*, 2012, **48**, 254-256.

116 B. Mu, P. M. Schoenecker and K. S. Walton, *J. Phys. Chem. C*, 2010, **114**, 6464-6471.

117 R. Serna-Guerrero, E. Dána, A. Sayari, *Ind. Eng. Chem. Res.*, 2008, **47**, 9406-9412.

118 T. Y. Ma and Z. Y. Yuan, *Eur. J. Inorg. Chem.*, 2010, **19**, 2941-2948.

119 T. Y. Ma, X. Z. Lin, X. J. Zhang and Z. Y. Yuan, *Nanoscale,* 2011, **3**, 1690-1696.

120 T. Y. Ma, X. Z. Lin, X. J. Zhang and Z. Y. Yuan, *New J. Chem.*, 2010, **34**, 1209-1216.

121 G. P. Knowles, S. W. Delaney and A. L. Chaffee, *Ind. Eng. Chem. Res.*, 2006, **45**, 2626-2633.

122 L. Liu, Q. F. Deng, X. X. Hou and Z. Y. Yuan, *J. Mater. Chem.*, 2012, **22**, 15540-15548.

123 X. -J. Wang, P. -Z. Li, Y. F. Chen, Q. Zhang, H. C. Zhang, X. X. Chan, R. Ganguly, Y. X. Li, J. W. Jiang and Y. L. Zhao, *Sci. Report*, 2013, **3**, 1-5.

124 K. Z. Hossain and L. Mercier, *Adv. Mater.*, 2002, **14**, 1053-1056.

125 H. L. Jiang, Y. Tatsu, Z.-H. Lu and Q. Xu, *J. Am. Chem. Soc.*, 2010, **132**, 5586-5587.

126 T. Y. Ma, X. J. Zhang, G. S. Shao, J. L. Cao and Z. Y. Yuan, *J. Phys. Chem. C*, **112**, 3090-3096.

127 B. O'Regan and M. Grätzel, *Nature*, 1991, **353**, 737-740.

128 J. Burschka, N. Pellet, S. -J. Moon, R. Humphry-Baker, P. Gao, M. K. Nazeeruddin and M. Grätzel, *Nature*, 2013, **499**, 316-320.

129 C. Wang, Z. G. Xie, K. E. deKrafft and W. B. Lin, *J. Am. Chem. Soc.*, 2011, **133**, 13445-13454.

130 M. Pramanik, M. Nandi, H. Uyama and A. Bhaumik, *Catal. Sci. Technol.*, 2012, **2**, 613-620.

131 A. Dutta, M. Pramanik, A. K. Patra, M. Nandi, H. Uyama and A. Bhaumik, *Chem. Commun.*, 2012, **48**, 6738-6740.

132 A. Corma, L. T. Nemeth, M. Renz and S. Valencia, *Nature*, 2001, **412**, 423-425.

133 X. Shi, J. Yang and Q. H. Yang, *Eur. J. Inorg. Chem.*, 2006, 1936-1939.

134 F. J. Song, C. Wang, J. M. Falkowski, L. Q. Ma and W. B. Lin, *J. Am. Chem. Soc.*, 2010, **132**, 15390-15398.

135 F. J. Song, C. Wang and W. B. Lin, *Chem. Commun.*, 2011, **47**, 8256-8258.

136 X. Z. Lin and Z. Y. Yuan, *Eur. J. Inorg. Chem.*, 2012, 2661-2664.

137 T. Y. Ma, L. Liu, Q. F. Deng, X. Z. Lin and Z. Y. Yuan, *Chem. Common.*, 2011, **47**, 6015-6017.

138 M. Cheng, E. B. Lobkovsky, G. W. Coates, *J. Am. Chem. Soc.*, 1998, 120, 11018–11019.

139 J. L. Song, Z. F. Zhang, S. Q. Hu, T. B. Wu, T. Jiang and B. X. Han, *Green Chem.*, 2009, **11**, 1031–1036.

140 O. V. Zalomaeva, A. M. Chibiryaev, K. A. Kovalenko, O. A. Kholdeeva, B. S. Balzhinimaev, V. P. Fedin, J. Catal., 2013, 298, 179–185.

141 J. Kim, S. N. Kim, H. G. Jang, G. Seo and W.S. Ahn, *Appl. Catal. A*, 2013, **453**, 175–180.

142 Y. Xie, T. T. Wang, X. H. Liu, K. Zou and W. Q. Deng, *Nat. Commun.*, 2013, DOI: 10.1038/ncomms2960.

143 J. L. Cao, Y. Wang, X. L. Yu, S. R. Wang, S. H. Wu and Z. Y. Yuan, *Appl. Catal. B*, 2008, **79**, 26-34.

144 S. Hudson, J. Cooney and E. Magner, *Angew. Chem. Int. Ed.*, 2008, **47**, 8582-8594.

145 V. Lykourinou, Y. Chen, X. -S. Wang, L. Meng, T. Hoang, L. -J. Ming, R. L. Musselman and S. Q. Ma, *J. Am. Chem. Soc.*, 2011, **133**, 10382-10385.

146 P. Horcajada, C. Serre, M. Vallet-Regí, M. Sebban, F. Taulelle and G. Férey, *Angew. Chem., Int. Ed.*, 2006, **45**, 5974-5978.

147 P. Horcajada, T. Chalati, C. Serre, B. Gillet, C. Sebrie, T. Baati, J. F. Eubank, D. Heurtaux, P. Clayette, C. Kreuz, J. S. Chang, Y. K. Hwang, V. Marsaud, P. N. Bories, L. Cynober, S. Gil, G. Férey, P. Couvreur and R. Gref, *Nat. Mater.*, 2010, **9**, 172-178

148 K. E. Uhrich, S. M. Cannizzaro, R. S. Langer and K. M. Shakesheff, *Chem. Rev.*, 1999, **99**, 3181-3198.

149 X. Shi, J. P. Li, Y. Tang and Q. H. Yang, *J. Mater. Chem.*, 2010, **20**, 6495-6504.

150 H. Li, T. Y. Ma, D. M. Kong and Z. Y. Yuan, *Analyst*, 2013, **138**, 1084-1090.